Cosmic Baby and Human Baby-Do Both of Them Exhibit a Similar Type Characteristics?: A Possibility

Ramen Kumar Parui [a] [*] [#]

[a] ARC, Room No-F101, Block-F, Mall Enclave,
13, K. B. Sarani, Kolkata-700080, India.
[*]Corresponding Author; email: rkplaruidr[at]yahoo.com
[#] ORCID No: 0000-0001-6838-3341

"Knowing is not enough, we must apply; Willing is not enough, we must do"-Geothe

Abstract: Recent discovery of earth like motion of the space-time implies that early or baby phase of compact objects may exhibit a similar type characteristic compared with that of baby phase of human or a similar type response on the same tests applied on both the cosmic baby and human baby cases. Triaxial shape appears in stellar compact object when it diverges from (Maclaurin) spheroidal shape to (Jacobian) ellipsoidal shape due an increase in rotation causing the compact object into a "Triaxial Star". In the case of formation of human baby, initial circular shape of the gestational sac turns into ellipsoidal shape due to its growth and as a result, it is suggested that the gestational sac would suffer "triaxial phase" which makes the human embryo to turn into a beautiful face and ageless appearance in women's body structure. Hourglass structure observed in cosmic objects and in human body shape. For cosmic objects such as supernova SN1987A, Planetary Nebula MyCn 18, Star forming region Lagoon nebula Hubble 12, protostar L1527, isolated pulsar PSR B1827-11, Magnetar, Cocoon inside a dying massive star, magnetic field in star forming region, Galaxy in the presence of black hole, variable stars etc. exhibit hourglass shape in their structure. In the case of human, we physically observe such hourglass shaped female body around us. Human mind expresses various mental states based on hourglass theory.

Time Reversal is another significant scenario that human embryo faces in its early phase while binary NS-NS and NS-BH mergers emit short gamma ray bursts as evidence of time reversal occurring.

Based on the above supporting phenomena this author suggests that;

i) Stars' babies and human babies both exhibit a similar type characteristic;
ii) Cosmic connection might be present in human that has not yet been discovered;
iii) These (in) direct evidences favour the origin of life in space;
iv) Triaxiality during embryo's early development phase might have a significant role towards the formation of hourglass body shape structure and ageless appearance in human body.

Keywords: Umbilical cord, cosmic baby, ultrasonography, clinical research

1.Introduction

A serendipitous happening was occurred in the early phase of life of Indian Scientist Jagadish Chandra Bose (known as J C Bose) when he observed through stepping on "Mimosa Pudica" (in Bengali-Lajjabati, meaning "shy one" or "shame plant") that this plant was folding of its leaves. This propelled him to do research throughout his life on an unanswered question-"Is there any possible relation between our own life (i.e. Human) and that of the plant world?"

In 1913, just before the beginning of the first World War I, J. C. Bose delivered a seminal speech entitled -" Plant Autograph and their Revelations" to the Royal Institution of UK for claiming the plants have living life, unfolding the hidden history in the life of plants: they response in storm and sunshine, in the warmth of summer and in the cold of winter, as well as in drought and rain, implying that they leave behind subtle impress under different situations [1]. Even plants also cry in distress condition like human [2].

In fact, Jagadish Chandra Bose was the first to prove that plants (on that time these considered as non-living objects) are like any other life form having a definite life cycle, a reproductive system, and also are aware of their surroundings [3].

In 1915 Einstein [4, 5] redefined matter relating to space-time as: "space-time tells matter how to move; matter tells space time how to curve" implying that when objects with mass, they should cause ripples that spread through space-time in the form of gravitational waves. These gravitational waves carry information of the source from which it is originated.

Recently, scientists have found evidence of the motion of the space-time [6] i.e. earth kind motion in the fabric of space-time wrapped by gravitational waves. This implies that the early or baby phase of compact objects in the sea of space-time have a similar characteristic with that of the baby phase of human on the earth. This means that there may have a responsive characteristic which are of similar type between the cosmic baby and earth based human baby.

In this paper I have attempted to find an answer of this problem. The paper is organised as follows: Sec.1 as introduction that deals with Jagadish Chandrs Bose's contribution to prove that trees (as a non-living object on that time) have a similar type response that of the living objects like human. Sect.2 describes the discovery of the motion of space-time and its significances. The details of the discovery of Cosmic Baby i.e. Swift J 1818.0-1607 having aged of 240 years and detection of a neo-natal Cosmic baby are covered in Sec.3. Different characteristics of human baby on the earth-Umbilical cord, heart Beat, cry, sneeze, twin, conjugate baby, USG images in 1st, 2nd, 3rd Trimester are described in Sec.4. Characteristics of cosmic baby in space -Umbilical cord, heartbeat, First cry, Sneeze, , binary, contact binaries, USG image i.e. echography etc are stated in Sec.5. The significance of this study i.e. new insights in the cosmic development and human development are described in particular the appearance of hourglass shape in various cosmic objects and hourglass shape in female body structure are described in Sec.5. Sec.7 covers the occurrence of time reversal scenarios in human embryo at the early phase of its evolution and emission of soft gamma ray bursts as evidence in NS-NS and NS-BH mergers. The concluding Sect.8 includes the author's suggesting ideas.

2.Discovery of the motion of Space-time

Albert Einstein predicted two facts in his general theory of relativity [4, 5] that;

(1) Gravitational waves that are ripples in space-time originated by massive accelerating objects;
(2) When a gravitational wave passes through space, it makes the space shrink and then expand periodically i.e. creation of a motion in space-time.

In 2015 scientists / astronomers were able to first detect directly the gravitational waves, originated from a binary balck holes, situated at 1.3 billion light years away from earth, through LIGO / VIRGO [6, 7].

For understanding and detecting of space-time ripples the NANOGrav ((North American Nanohertz Observatory for Gravitational Waves) collaboration team [8] considered those pulsars that;

(a) Rotate extremely fast i.e. up to 1000 times per second, and
(b) Those pulses that can be timed like "the ticking" of an extremely accurate cosmic clock.

Now, when the gravitational waves sweep or cross a pulsar at the speed of light these gravitational waves will expand very little and then contract the space-time distance between the pulsars and the earth. As a result, a very slightly changing between the ticks. Observed data analysis show that pulsars are such accurate clocks through which it is possible to measure their ticking with an accuracy to within 100 nanoseconds. As the distance between a pulsar and earth is ~ 100 feet (i.e.300 meters) so any change in distance (~ tens of miles) between the pulsars and earth due to gravitational waves, making pulsars sensitive enough to detect this effect easily.

Recently, the NANOGrav collaboration team was able to detect a "hum" [9] (i.e. some disruption in the ticking of one pulsar arises due to gravitational wave from the distance universe). When the team was analysing the observed parameters of 68 different pulsars for a period of 15 years. According to them this "hum" is the presence of a low frequency gravitational wave background and this signal is coming from a population of super massive black hole (SMBH) binaries distributed throughout the universe. In fact, there are many physical processes that are comparable of producing such low frequency gravitational waves. But their analysis was based on the strong observational evidences which suggest that;

(i) Most of the massive galaxies, not all, have supermassive black holes at their centers [10];
(ii) Hierarchical structure formation supports frequent galaxy mergers [11, 12].
(iii) This frequent galaxy merger, ultimately leads to the formation of supermassive black holes (SMBHs) binaries as well as merging of SMBHs binaries [13].
(iv) Strong nanohertz gravitational waves are produced and emitted at the last stages of merger of SMBH binaries.

In the conclusion the NANOGrav team remarks that they are not yet able to confirm that SMBHs binaries are only the origin of the low frequency gravitational waves background. The significance of their finding a "hum" that shows the evidence of the presence of a low frequency gravitational wave background i.e. the motion of the space-time.

3.Discovery of Cosmic Baby

On 12th March 2020 at 21: 16: 49 UTC Swift Observatory [14] detected a typical characteristic of a short burst from a magnetar [15]. Finally, this was a new, uncatalogued X-ray source namely Swift J1818.0-1607 (presently known as Cosmic Baby). Different important parameters of this cosmic baby, as estimated from the observed data, are:

Characteristic age ~ 240 years [16]
Coherent periodicity of X-ray signal 1.36 s [17]
Surface magnetic field ~ 2.7 x 10^{14} G
Dipolar magnetic field at poles ~ 7 x 10^{14} G
Spin period 0.7333920 s
Spin period derivative ~ 8.2 x 10^{-11} s. s^{-1} [18]

In fact, following a series of observations through different telescope at several wavelength till 27th July 2020 the confirmed parameters of this magnetar (i.. cosmic baby) were:

Rotation or spin period derivative ~ 3.74 x 10^{-11} s^{-2}
Surface dipole magnetic field 3 x 10^{14} G
Spin down luminosity ~ 1.1 x 10^{36} erg. s^{-1}
and so on.

Based on the observed data Parui [19-21] estimated:

(i) Cosmic Baby's Internal core magnetic field (B_{int}) ~ 8.9424 x 10^{17} G,
(ii) Ellipticity ~ 9 x $10^{-3,}$
(iii) It is a triaxial star in nature and will exhibit its triaxial nature for a period of at least 700-760 years.

Magnetars are considered as a rare class of relativistic slow rotating neutron stars possessing very strong magnetic fields. The Swift J 1818.0-1607 is a baby magnetar of characteristic age of ~ 240-300 years having very strong internal core magnetic field of ~ 8.9424 x 10^{17}G. As the characteristic age of this cosmic baby is only ~ 240-300 years i.e. the baby phase still compared to thousands of years, it will definitely exhibit triaxility i.e. triaxial behavior at least up to its age 1000 years. This means that the estimated ellipticity of this cosmic baby (i.e. 9 x10-$^{3)}$ lies within the range for triaxiality which will remain almost at that value for exhibiting a triaxial nature for at least 700-760 years [20]. In other words, this cosmic baby can be considered as baby triaxial star with age of ~ 240-300 years.

NeoNatal Cosmic Baby

In a study of reanalyzing the available earlier observed data of GRB 130310A Zhang et al [22] estimated the age of the magnetar associated with this gamma ray burst (GRB) is two weeks only. The available observed parameters of the associated magnetar after a time span of 2 weeks are:

Period ~ 80ms
Dipolar magnetic field strength ~ 10^{14}-10^{15} G
Internal magnetic field could be as high as ~ 10^{17} G.

Based on the findings of Zhang et al [22] and available observed data Parui [23] estimated the interior magnetic field strength and ellipticity of the millisecond magnetar associated with the GRB 130310A are ~ [1.25 (lower), 3.995 (highest)] x 10^{17} G and (1.25, 3.995) x 10-^{3,} respectively. As the ambipolar diffusion is active which prevents both the decay of the interior magnetic fields and cooling of the magnetar such that magnetar core temperature remains higher than several times 10^{8} K for a period of a few thousand years (at least 10^{3} years), Parui proposed that the nature of this newly born magnetar associated with GRB130310A is triaxial type i.e. "Neo Natal Triaxial Star" [24].

4.Characteristics of New Born Human Baby

After fertilization about 40 weeks is required for the birth of newly baby. During the stay of 40 weeks inside the mother's womb various phase change has to face towards turning of an egg into full baby form. Even after birth the newly born baby also crosses different phases. The various significant phases are discussed below:

4.1 Umbilical Cord

The umbilical cord is a tube that vitally connects a baby (i.e. fetus) to its mother's placenta during pregnancy. It is a virtual lifeline for supplying the baby with oxygen and nutrients and removes waste products from the baby's circulation. Not only that this cord also serves as a physical and emotional connection between the mother and fetus. The umbilical cord begins to develop around week 3 and fully formed by week 7. The origin of the umbilical cord arises from and contains remnant of the

yolk sac and allantois. Actually, it forms from the 5th week of development when the yolk sac is replaced as the source of nutrients for the embryo [25].

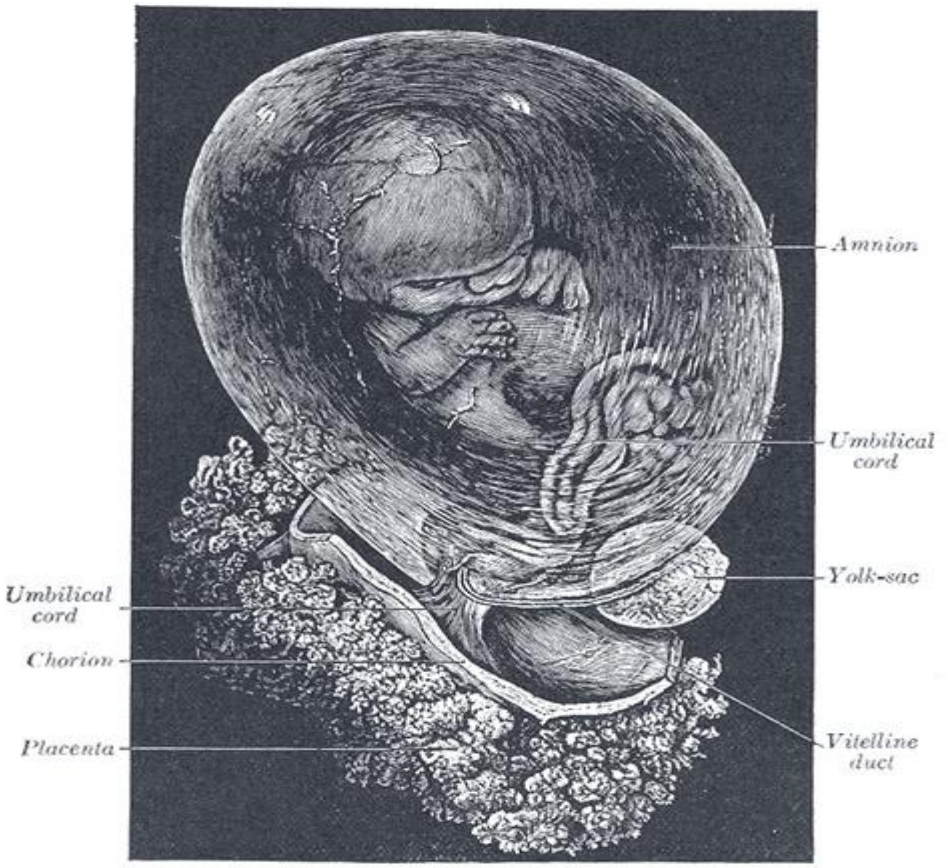

Figure 1: Schematic diagram shows the development of the Fetal Membranes and Placenta. The fetus is approximately 8 weeks enclosed in the amnion (Courtesy: Henry Vandyke Carter, Public Domain, via Wikimedia Commons)

It has been observed from the ultrasonography of an embryo of a gestational age of 8 weeks and 3 days that the embryo is surrounded by the thin membrane of the amniotic sac within which the umbilical cord located at the center, attaching the embryo to the placenta [26, 27].

The umbilical cord contains jelly i.e. a gelatinous substance produced largely from mucopolysaccharides which protects the blood vessels inside it. In general, this umbilical cord contains one vein (carries oxygenated, nutrients-rich blood to the fetus) and two arteries that carry de-oxygeneted, nutrient depleted blood away [26]. Usually, the length of the umbilical cord is about 50 cm (i.e.20 inch) long (that is approximately equal to the crown-rump length of the fetus) and about 2 cm (i.e.0.75 inch) in diameter. The blood flow through the umbilical cord is [28, 29]:

(a) Approx.35 ml/min at 20 weeks (i.e.115 ml/min/kg at 20 weeks adopting the weight of fetus);
(b) Approx.240 ml/min at 40 weeks (i.e.64 ml/min/kg at 40 weeks adopting the weight of fetus).

After birth, this cord is clamped and cut, leaving a short piece (called stump) attached to the baby's belly bottom. In fact, this stamp will dry up naturally and fallen down within a few weeks.

4.2 Heart Beat

In the case of a human baby heart is the embryo's first functional organ and its development starts as early as 16 days after fertilization [30]. In order to the embryo's survival matter the heart form very early so that circulation of oxygen carrying blood begins. Actually, the cardiac tissue begins to pulse at around 5-6 weeks of pregnancy. This heart beat can be observed through Ultrasonography (USG) although the heart not yet developed [31].

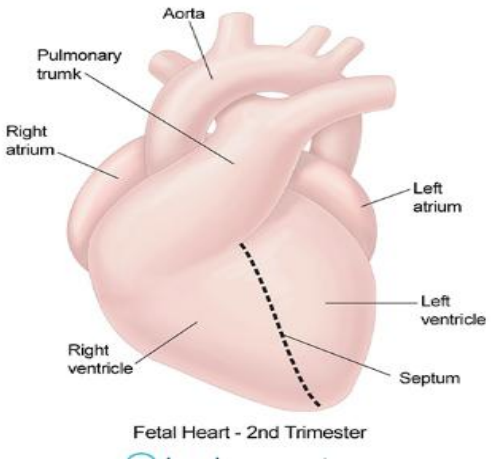

(A)

(B)

Figure 2: Schematic diagram showing Fetal Heart at 2nd Trimester (i.e.13-27 weeks) (A), and (B) image of Fetal Heart obtained in a ultrasound of an embryo at 6-week age (image credit: iStock / Getty Images Plus)

Week 6 -in this time dramatic change will occur in the heart of the embryo and the basic heart tube turns into a loop shape i.e. forming an "S" shape.

Week 7-pumping chambers i.e. ventricles and receiving chambers or atria of the heart begin to separate and develop gradually.

Week 8-formation of the valves between the atria and ventricles takes place.

Week 9, 10-the aorta and pulmonary vain form that indicates the fetal heart has matured i.e. developed fully.

Note that through ultrasound the cardiac contraction will be visible and observed facts of a human baby's heart beat rate, in general, are:

(i) During the first month: starting at around 75-80 beats per minute (BPM) and the highest at 165-185 BPM at the 7th week.
(ii) This rate is accelerated by around 3.3 BPM per day or 10 BPM every three days.
(iii) After attaining the peak, the heart beat rate decelerates, reaching an average of 145 BPM.
(iv) With the development or growth of the fetus this rate comes to 110-160 BPM.

4.3 Ultrasonography Images

Ultrasonography (or Sonogram) is a test during pregnancy i.e. prenatal ultrasound checks on the health and development of the growing baby inside the mother's womb. During an ultrasonography (USG) sound wave is used which transform into image that can be seen on a screen. In general, the pregnancy period of 40 weeks is divided into three i.e.

First Trimester-week 1 to week 12,
Second Trimester-week 13 to week 28,

Third Trimester-week 29 to week 40.

In each trimester the fetus develops and meets specific developmental milestones that can be checked from the USG imaging. In pregnancy the first trimester i.e. the first 12 weeks is a crucial time for fetal development. As per conception, a zygote is formed from the combination of the egg and sperm. This zygote becomes an embryo at its cell division progresses and grows [33].

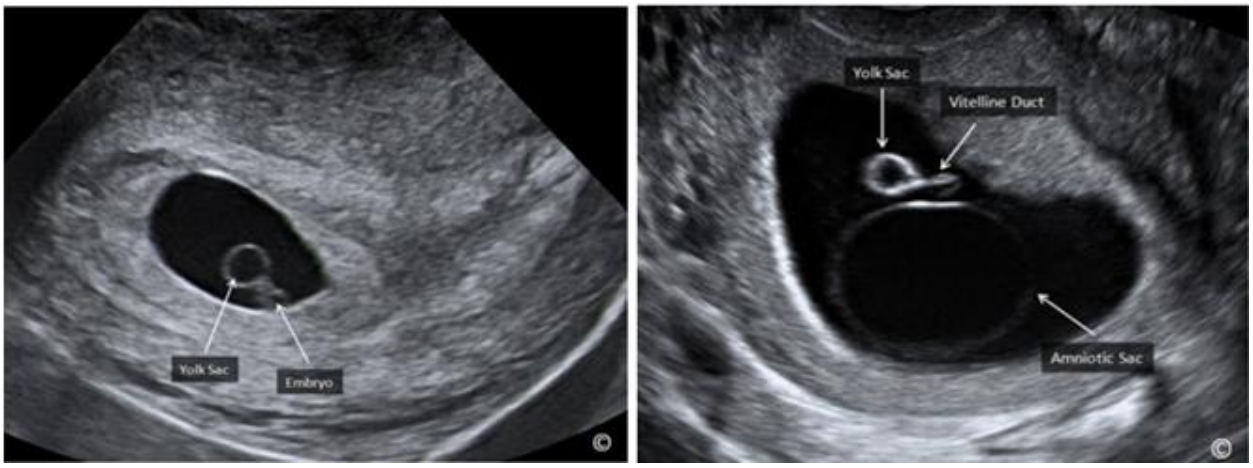

(A) Mid sagittal plane of a uterus with a gestational sac at 6 weeks' **(B)** Gestational sac at 7 weeks gestation. Amionic sac gestation. A yolk sac (labelled) and a small embryo (labelled) is looking like a thin reflective circular membrane. Extra-**Note that the shape of the gestational sac is more ellipsoid** amniotic structure is also seen (labelled) than circular

(C) Gestational Sac with an embryo at 8 weeks. Body curvature is **(D)** Gestational sac with an embryo at 10 weeks gestation. Head, also seen. Embryo and Yolk sac are labelled. Chest, Abdomen and extremities are also clearly seen.

Figure 3: Various USG images of gestational Sac with different aged embryo (adopted from ref [32], Courtesy: Global Library of Women's Medicine)

At the end of the first trimester (i.e. 12 weeks) the significant developed body parts are (see Figure 3A-D):

- Major organs and structures of the body have begun to develop
- The fetus is around 3 inches in long and weight ~ 1 ounce
- The heart is beating regularly
- Finger and toes have formed, nerves and muscles work together
- The eye lids have formed but will remain closed.

Note: the clear delineation of a head, chest, abdomen and extremities. CRL=Crown-Rump Length.

The significant noticeable fact is the Ellipsoidal shape of the Gestational Sac (figure 3A).

4.4 Ellipsoidal Shape of the Gestational Sac

The gestational sac (also known as chorionic cavity) if first located slightly paracentically in the decidua. It has a rapid growth at about 1 mm per day. When the gestational sac has a mean diameter of 2-4 mm its borders appear echogenic. The ultrasonographic image of gestational sac at week 5 (approx.) is shown in figure 4. The embryo is surrounded by a large

cavity of fluid, known as gestational sac. This sac is normally located within the uterus and can be seen by USG. Initially the shape of the gestational sac is circular but with the appearance of the yolk sac and **the embryo it becomes more ellipsoid.**

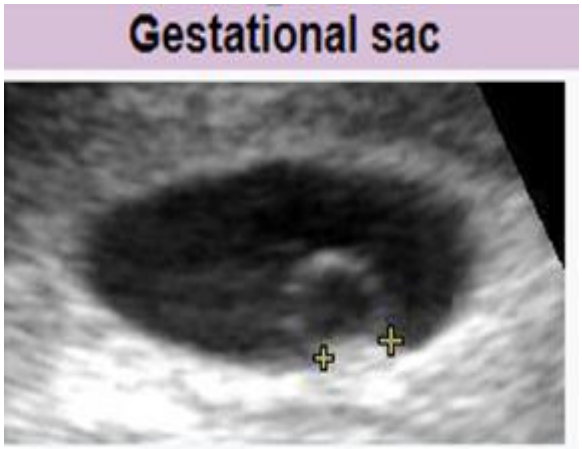

(A)

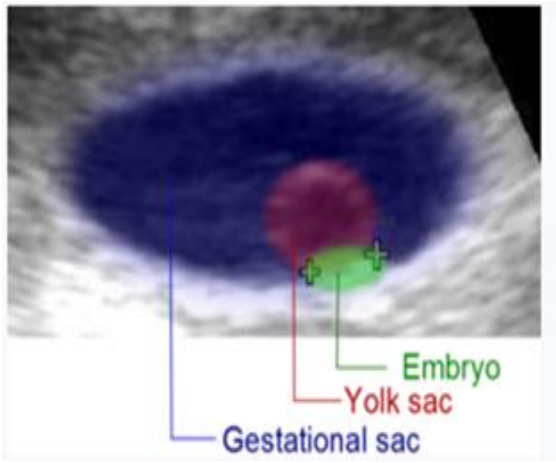

(B)

Figure 4: Enlarged version of USG image of gestational sac. **(A)** The contents inside the cavity of the uterus at approx.5 weeks of Gentational sac **(B)** Artificially coloured showing gestational sac (dark blue), yolk sac (red) and embryo (green). The distance between the + sign is 3 mm. Ellipsoid shape of the gestational sac is clearly viewed. (adopted from Wikipedia)
At the end of second Trimester (i.e. 28 weeks) (Figure 5 A-G)

By the end of the 2nd trimester the developed parts of a human baby have been observed through USG are:

- the fetus can see, hear
- the fetus movement i.e. sucking motion and scratch, regular sleeping, waking
- skin, hair, nails have formed
- Bone marrow is making blood cells
- Male's testicles and female's egg have formed

(A): USG image of Biparietal diameter plane.1 Biparietal diameter 2 Cavum Septum pellucidum 3 Thalami 4 Hypoechoic skull sutures 5 Third Ventricle 6 Choroid 7 Posterior Lateral ventricle 8 Corpus callosum

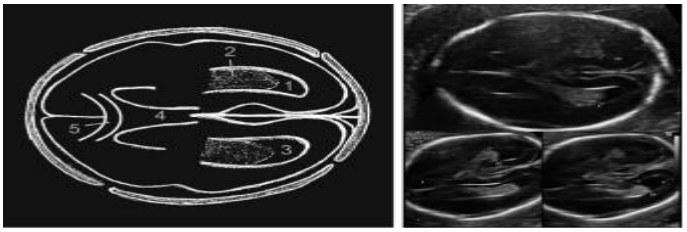

(B): USG image of Transventricular plane. The lower right images demonstrate that angling the fetal head can improve visualisation of the near field lateral ventricle.1 Near field posterior horn of lateral ventricle 2 Choroid 3 Far field posterior horn of lateral ventricle 4 Cavum Septum Pellucidum (CSP) 5 Corpus callosum (CC)

(C): USG image Corpus callosum.1 Corpus callosum 2 Cavum Septum Pellucidum 3 Nasal bone

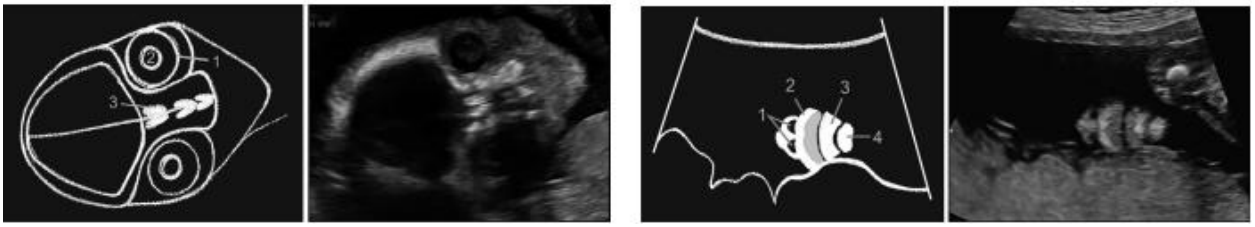

(D): USG image of Coronal Orbits.1 Orbit 2 Lens of the eye 3 Nasal bridge (E) Coronal lips and nose 1 Two nostrils 2 Upper lip 3 Lower lip 4 Chin

(F): USG image of Axial orbit and lenses.1 Orbit 2 Lens 3 Nasal bridge (G) USG Profile and nasal bone 1 Nasal bone 2 Nose 3 Mandible 4 Hard palate

Figure 5: Various body parts developed of a human baby as obtained in USG images during the period week 13-28 (adopted from ref [34], Courtesy: AJUM)

At the end of 3rd trimester (i.e. from week 29 to till delivery (see Figure 6 A-G)

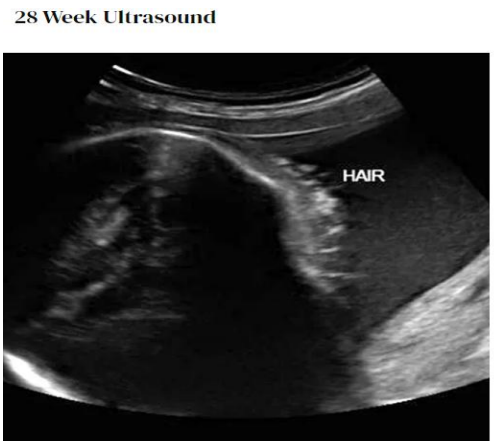

(A) USG image showing baby's hair waiving in amniotic fluid. **Fetal Size:** Length, 10 inches, crown to rump; total length 15 3/4 inches. Weight, almost 2 1/2 pounds; Developed body parts: Brain tissue, scalp hair, eyes are open, weight gaining. This hair is also called Lanugo.

(B) USG image as observed at 29 weeks indicating baby's bones are hardening, muscles are strengthening. Bones appear as bright white. **Fetal Size:** Length, 10 1/2 inches, crown to rump; total length 16 3/4 inches. Weight, 2 3/4 pounds

(C) At a 30 week USG image shows how the baby is developing with pouty lips, tiny nose, eyes, forehead. Fetal Size: Length, 10 3/4 inches, crown to rump; total length 17 inches. Weight, 3 pounds.

(D) USG image shows brain is continuing to grow and develop. In this image, the red and blue show blood flow to the part of his brain that lets the two halves of the brain communicate with one another.

(E) USG image gives a close-up view of the lower end of your unborn baby's spine. **Fetal Size:** Length, 11 3/4 inches, crown to rump; total length almost 18 inches. Weight, 3 1/2 pounds.

(F) USG image at 40 week showing cross-section of the baby's belly. The small back oval of their stomach, and the curved black line is the blood vessel that brings nutrients from the placenta.

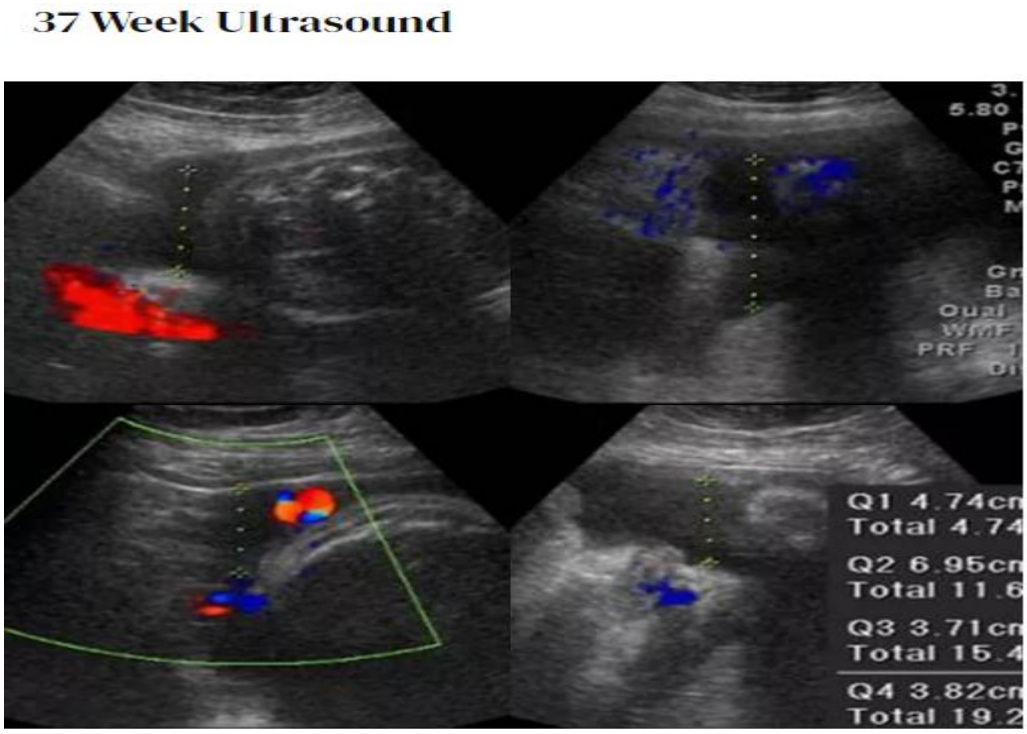

(G) USG image at 37 weeks indicating the baby is in full term! one of the most important measurements the sonographer can take is abdominal circumference. Fetal Size**:** Length, 14 inches, crown to rump; total length 21 inches. Weight, 6 1/2 pounds
Figure 6: Various body parts developed of a human baby as obtained in USG images during the period week 29-40 (adopted from ref [35], Courtesy: American Institute of Ultrasound in Medicine-AIUM. org)

During this 3rd trimester almost all organs and body systems have formed but these are continuing to grow and mature. The significance body parts are [36]:

- Lung formation becomes complete
- Body movements are noticeable, eyes are open and sense light
- The bones are hardening

●The fetus drops lower in the abdomen and usually head down position

USG imaging of the fetus from the formation of embryo to the delivery of the baby plays a vital role. This imaging also enables us to see the development of the fetus for knowing the health and required developments for good health, any abnormality, etc. In brief, the main aim of the USG is to utilize during the 1st and 2nd trimester to establish the gestational age of the pregnancy and eventually to evaluate fetal anatomy.

4.5 Twin Baby

First trimester is the most optimum time for diagnosis of single or twin or multiple gestations as well as for the assessment of chorionicity. For twins, as per USG imaging observations, there are;

Figure 7: USG image of (**A**) Monochorionic-diamniotic twins (A and B) at 8 weeks gestation (presence of 2 yolk sac (arrows) are visible but separating membrane is not visible)

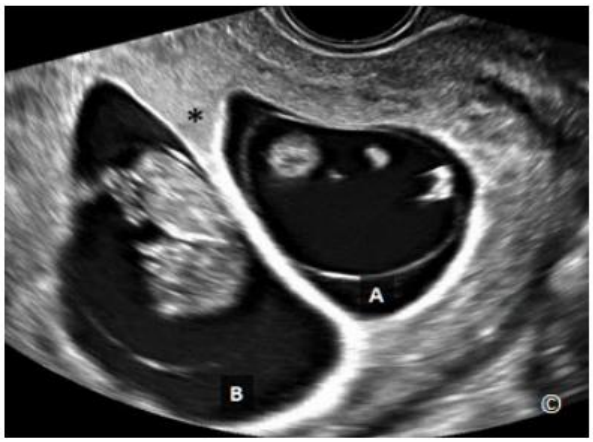

(**B**) Dichorionic-diamniotic twin pregnancy. (noticeable is the thick dividing membrane separating both gestational sacs A and B) (adopted from ref. [32], Courtesy: GLWM)

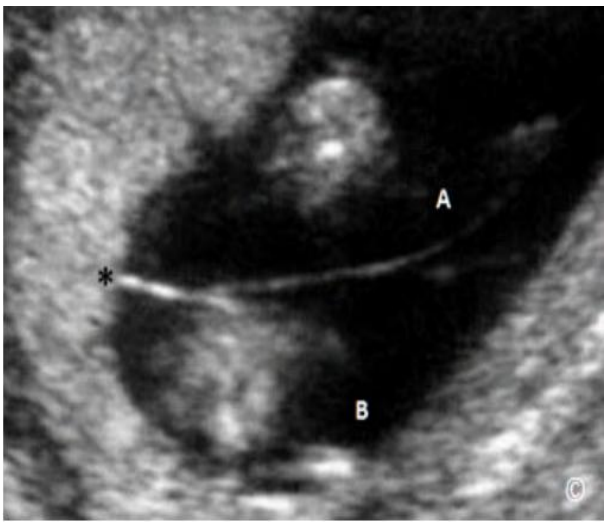

Figure 7: (C) USG image of Monochorionic-Diamniotic twins showing a thin dividing membrane that separates the amniotic cavities (A and B) and inserts in a characteristic "T" configuration (asterisk) into the shared placenta.

(**D**) Monochorionic-monoamniotic twins (A and B). Note the presence of a single amniotic sac (labeled). (Adopted from ref [32]. COURTESY: GLWM) two possibilities: (a) it can share one placenta and referred as Monochorionic (MC), or (b) can have two separate placentas, called Dochorionic (DC). Thus, all the dichorionic placentas have 2 amnionic sacs, i.e., dizygotic twin always has dichorionic placenta. Not only that, dizygotic twins are more common than monzygotic twins.

4.6 Conjugate Baby

Conjugate twins are monoamniotic, and these twins are best diagnosed in the early gestation after 8 weeks when yolk sac is present. This type twins are sub grouped into three:

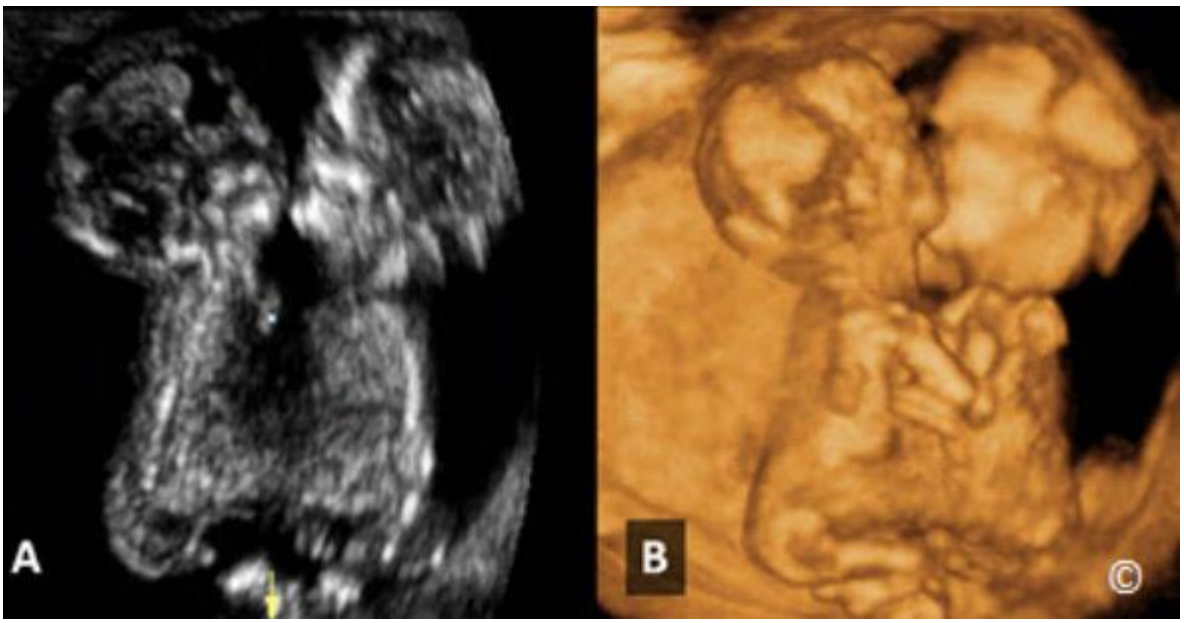

Figure 8: USG images of a Conjoined twins at 12 weeks gestation as observed on 2D (A) and 3D (B) ultrasound. Note that the twins are joined at the chest and abdomen. (adopted from ref. [32], Courtesy: GLWM)

1) Monochorionic-Monoamniotic twins: it contains one gestational sac, one amniotic sac but two embryos. No separating / dividing membrane.
2) Monochorionic-diamniotic twins: in this case there is one gestational sace but each embryo has its own amniotic sac and yolk sac. The amniotic cavaties are separated by a thin, "T" shaped configuration into the shared placenta.
3) Dichorionic-diamniotic twins: in this case there are two gestational sac divided by thich membrane that includes chorionic tissue.

4.7 Physical realistic Observations

First Cry

Birth of a human body means that the first minute of life which is called one of the most dangerous. Because during those 60 seconds an infant must inhale for the first time resulting which millions of tiny air sacks to open and then fill with air. Although all babies are different but most of the newborns do it naturally and quickly. So, the baby's cry indicates a healthy star of respiration. For this reason, an eagerly await of the baby's first cry in the labor and delivery room because it signals the newborn's ability to breath on its own. In other words, crying is synonymous with breathing. The significance of first cry is that it initiates successful transition from fetal circulation (when baby is inside the mother's womb and completely dependent on the mother and placenta for gas exchange) to outside the womb when baby must use its own lungs to sustain.

Sneezing, Noisy Breathing

Newborns spend most of their time sleeping, sometimes even when you are trying to feed them. They also grunt, grimace, squirm, kick, and startle easily, all of which are normal. Sneezing is the only way they can clear their nose and does not mean a cold has developed. Babies also breathe noisily and irregularly. This becomes particularly noticeable between three and six weeks of age. Nasal congestion is normal, and we suggest obtaining a rubber bulb syringe to help clear the mucus from the nose. Hiccoughs are frequent and go away by themselves.

Eye

In human eye the optic nerves is composed of retinal ganglion cell axons and glia. Again, each optic nerve contains nerve fibers counting between 7, 70, 000 and 1.7 million nerve fibers which form axons of the retinal ganglion cells of one retina. The ganglion cells, in the fovea, is as few as 5 photoreceptor cells where as these connect to thousands of photoreceptors like a network, in the other areas of the retina (Figure 9).

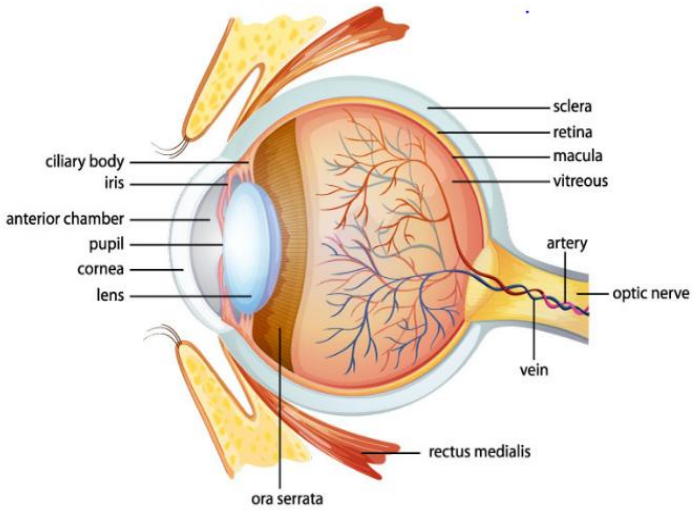

Figure 9: Schematic diagram nerves network in human eye (Image Credit: Chaedick optical)

5.Characteristics of Cosmic baby

5.1 Formation of a baby star and its umbilical cord

It is believed that supermassive black holes are located at the heart of every giant galaxy [37, 38]. Based on this idea and in order to search the compact radio source at the active, dynamical galactic centre of the dwarf galaxy Henize2-10 what they observed is the black hole driven outflows that plays an important role in heating and expelling gas. In fact, as a distance of approximately 9 Mpc, i.e. the central region of the Henize 2-10, a massive black hole is located and evidence suggests that the central black hole outflows influencing the star formation. From the optical observation of Henize2-10 Schutte and Reines [38] found an approximately 150pc long ionized filament that connects the region between the black hole and the site of star forming region. Analysis of their observed data hints that a supermassive black hole, which is located approximately 34 x 10^6 light years away in the galaxy Henize 2-10, was spewing an enormous, ionized gas in the form of a jet of 500 light yearlong from its center at a speed of 1.6 million kn/hour. This jet actually functioning as a "fire-strom" of new star or baby star formation in a nearby stellar nursery. According to them, this spotted super-massive black hole "giving birth" to baby stars which are tethered (i.e. rope or chain) to the black hole by a massive "Umbilical Cord" made of gas and dust. The significance of this finding is that this is first a black hole has been seen birthing baby star in a dwarf galaxy containing 1 billion or fewer stars galaxy, astronomers recently observed star formation at the active galactic center of the dwarf galaxy

Henize 2-10. What they observed is a black hole driven outflows that plays an important role in heating and expelling gas. In fact, at a distance of approx.9 MPc, i.e. central region of the Henize 2-10, a massive black hole is located and evidence suggests that the central black hole outflows influencing the star formation. From the optical observation of Henize 2-10 Schutte and Reines [38] found an approximately 150 Pc long ionized filament that connects the region between the black hole and the site of star forming region.

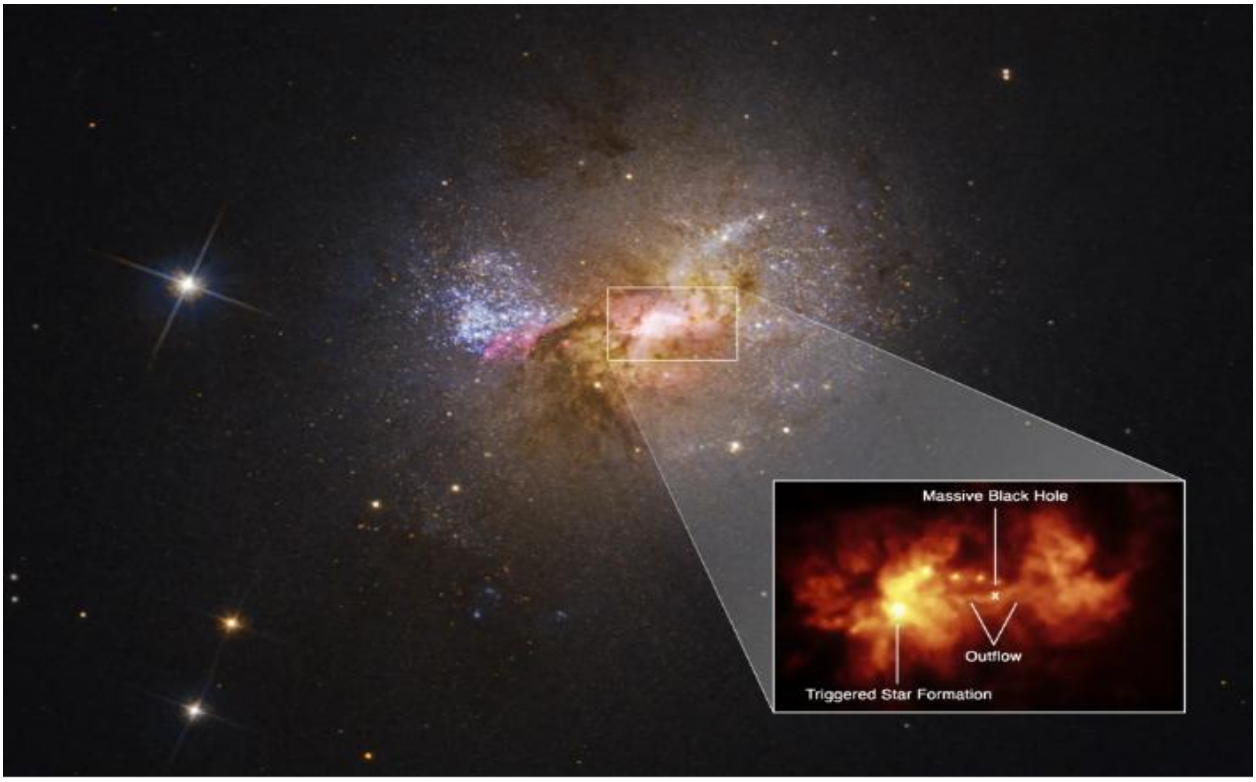

Figure 10: A Supermassive Black hole was detected at the center of the dwarf galaxy Henize 2-10 (Adopted from ref Schutte and Reines [38]; Image credit-NASA, ESA, Zachary Schutte (XGI), Amy Reines (XGI); Image Processing: Alyssa Pagan (STScI))

Analysis of their observed data hints that a super massive black hole, which is located approx.34 million light years away in the galaxy Henize 2-10, was spewing an enormous, ionized gas in the form of jet of 500 lightyear long from its center at a speed of 1.6m million km/hour. This jet actually functioning as a “firestorm” of new star or baby star formation in a nearby stellar nursery.

According to them this spotted supermassive black hole “giving birth” to baby stars which are tethered (i.e. rope or chain) to the black hole by a massive “umbilical cord” made of gas and dust. The significance of this finding is that this is the first a black hole has been seen birthing baby star in a dwarf galaxy containing 1 billion or fewer stars.

5.2 Heart Beat

Black holes are extreme compact objects that are alive. But very few black holes are there i.e. a tiny fraction of our known black holes which in turns out that they are alive and can have heart beats. When these tiny fraction black holes consume enomous amount of gas, emit x-ray signals on that time it resembles a human heart beat. These type black holes are in a binary system sharing an orbit with another star and they can pull in gas from its companion star. What happens in this case is that the pulling gas compresses and heat s up, possesses an incredible high temperature such that copious amount of x-ray binaries can show variability over multiple time scales i.e. undergoing recurrent outbursts lasting from months to years.

Figure 10: A Hubble Space Telescope image of a supermassive black hole at its center (Image credit: NASA/ESA/STScI)

Recently, astronomers observed through a phase-resolved view of "Heart Beat" like variability in IGR J17091-3624 [39]. Utilizing the data available from the NICER and NuSTAR space observatories they studied the x-ray outbursts variability of IGR J17091-3624 during its 2022 outbursts and found variation in spectral shape, in particular exhibiting significant synchronous variations in the disk temperature and flux with the count rate. This means that a positive correlation between the disk temperature and flux over the flare cycle but differs from a loop relation suggesting a difference in underlying physical processes between two variability classes with anticorrelation. This is similar one that vins and arteries perform their action in human heart.

5.3 Ultrasonography of Baby Star

By checking heart beats of a human baby by stethoscope doctor can easily realize internal health condition and through ultrasonography the functions of organs like heart, lungs, etc. Recently, an international team of astronomers [40] announced that they are able to monitor the heartbeat of a baby star with the help of two space telescopes i.e. Canadian MOST satellite and French CoRoT mission. Analysis of the observed data enables the scientists/ astronomers to understand the internal structures and ages of young stars, which allows them to check the evolution of our suni.e. the theories of how our sun appeared 4.5 billion years ago.

Like ultrasonography in case of human baby, they have performed ultrasonography of stellar embryo. As the stars can vibrate due to bouncing inside produced by sound waves, so sound vibration across the vacuum of space is capable to create a subtle change in stellar luminosity (i.e. brightness). Thus, decoding the frequencies of those vibrations ultimately offer the astronomers to relocate the hidden interior structure of the stars. The technique used by them is called "Echography" and they used this for observation of young clusters such as NGC 2264. The decoding of their result is represented in figure 11. The significance of their results clearly indicates the "dependency"-when a star begins to form i.e. at the suitable initial stage of formation from the ignition of thermonuclear fusion (which is similar to the first trimester of a human pregnancy) it pulses slowly.

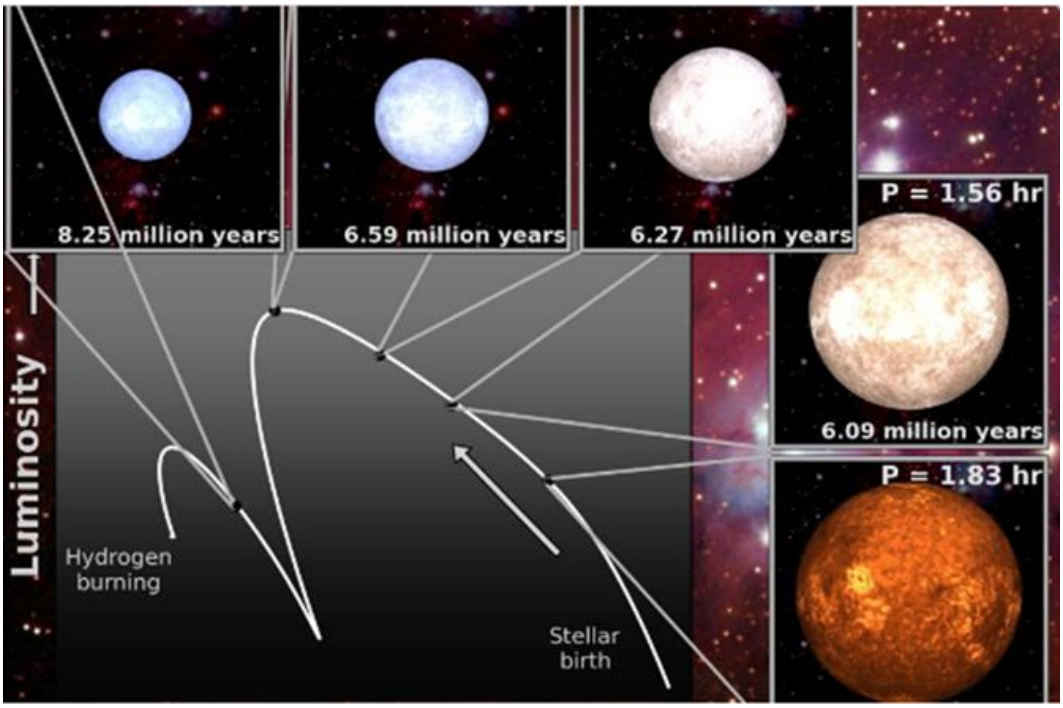

Figure 11: Schematic diagram (not scaled) showing the model of a composite image with detailing the pre-life story of a star like the sun as obtained by Zwinty et al [40]

The ignition of thermonuclear fusion at the star's core indicating to become a true star (the similar to the moment of birth of a human baby at the end of the third trimester) it pulses very faster. To monitor the pregnancy, its growth doctors observe through ultrasonography and record the size and weight of an embryo in the mother's womb. In the case of stars, to observe the star birth and its evolution astronomers, using echography, track the temperature and energy output (i.e. luminosity) of stellar embryo inside the star-forming region of a galaxy. According to the animated model, based on the animated data, shows that;

(a) In the pre-life story of a star like the sun-spinning time period ~ 10 million years from the conceive to birth;
(b) The stellar embryo vibrates with different rates at different points during its evolutionary phases / paths.
(c) Measuring the heart beats of the real baby stars and applying the measured data astronomers enable to make a possible theoretical model of a stellar evolution from embryo formation to birth of a star (most space telescope [14]).

5.4 Elliptical shape in star's birth phase

Very fast rotation and strong magnetic field inside a star deform from its spheroidal shape to ellipsoidal shape. For example-rotating neutron stars, isolated slow rotating neutron star with strong magnetic field i.e. magnetars are in deformed phased i.e. ellipsoidal shape. In case of binary system at least half of the detected solar type stars are in binary system. Although the formation mechanism of binary system is still debated but astronomers believe that pro-stellar phases, as there is a significant mass reservoir available in this phase, are the most ideal sources that have not undergone significant evolutionary path. In an observational study of three young proto-starsnLM1165-SMM1, L1157-mm, and CB230 IRS1 in the cepheus clouds, using very large array (VLA), Tobin et al [42] found that L1165-SMM1 and CB230 IRS1 have probably binary companions and position angle of these companions are nearly orthogonal to the direction of the observed bipolar outflows. They suggested that these companions may have formed from disk fragmentation with turbulent. It is also suggested that proto-star CB230IRS1 was formed after the spinning disk fragmentation and congealed into a star.

5.5 Binary stars like human fraternal twins

In fact, about half of all sun-like stars in the galaxy are binary stars but their evolution i.e. how these binaries form and grow up is not clear. The main argument is:

(a) Binaries are like twins, whether identical or not i.e. Beginning of their existence as a single entity and then divided into two early one, or
(b) Fraternal i.e. From scratch both forming in the same proto-stellar disk.
(c) Although another possibility is initially, they were separate, identical migrate across the interstellar space and then came into binary until the gravity joins them.

However, recent observation of L1165 dark cloud with the help of Herchel PACS and SPIRE photometers (see Figure 12) suggest that in some cases the twin model of binary star is appropriate or correct [43, 44].

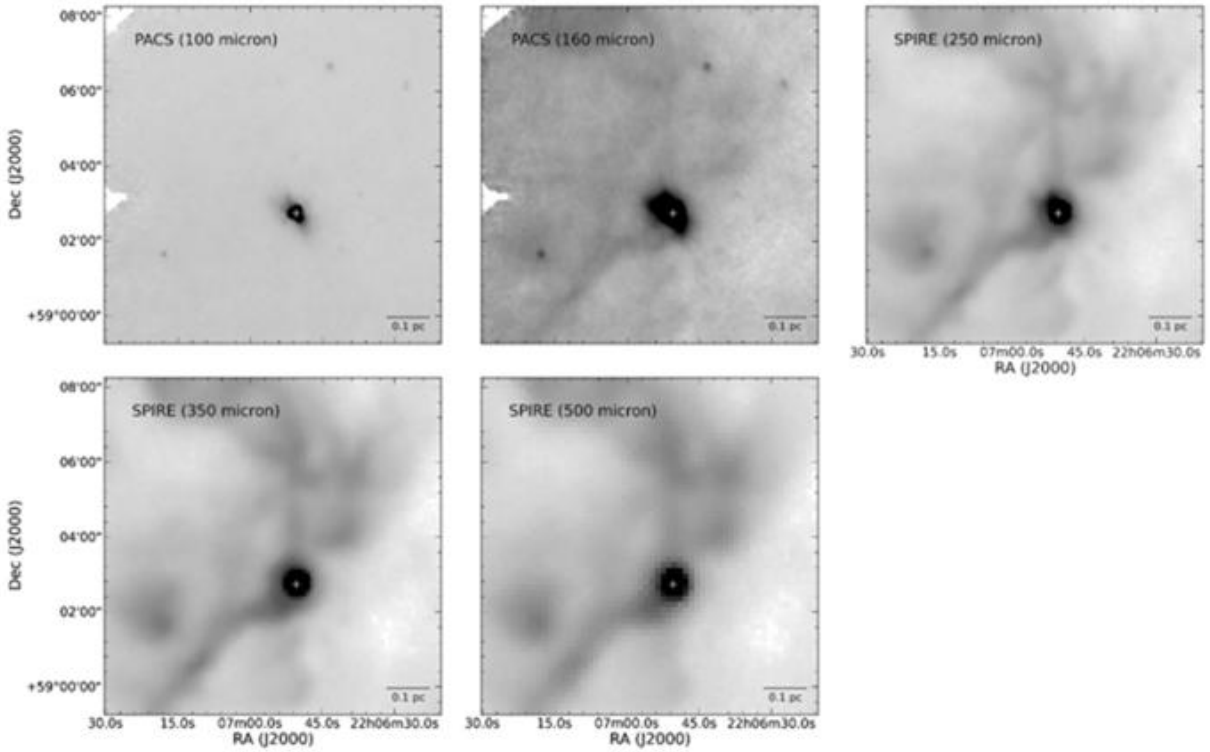

Figure 12: Observed snapshot of L1165 Herschel maps at 100 m, 160 m, 250 m, 350 m and 500 m. Note that the bright source L1165-SMM1 marked with a white cross in each case (adopted from ref [42])

5.6 Contact Binary like human conjugate twin

In the astronomical view a contact binary is a binary star system in which the component star is so very close such that they touch each other or have merged resulting which sharing of their gaseous envelopes. In this case, as the stars of the binary system share an envelope, they are also called over contact binary [44, 45]. Both the stars in these contact binaries have filled their Roche lobes which allow the more massive primary star component can transfer both mass and luminosity to the secondary component star. The significance is that both the components in a contact binary system exhibit similar effective temperature and luminosity, regardless of their respective masses. For example: W Ursae Majories [46].

This is a similar one when one conjugate human baby suffers, the other one also suffers from same disease.

5.7 Eye of a baby star

Figure 13 shows a model of the sun's magnetic field lines swirling out of its surface as appeared in the computer-enhanced ultraviolet snapshot. Each white line represents a powerful electromagnetic eruption arises due to high-energy interactions between the ultrahot, supercharged particles that make up both the sun's magnetic field and the plasma writhing around the star's surface.

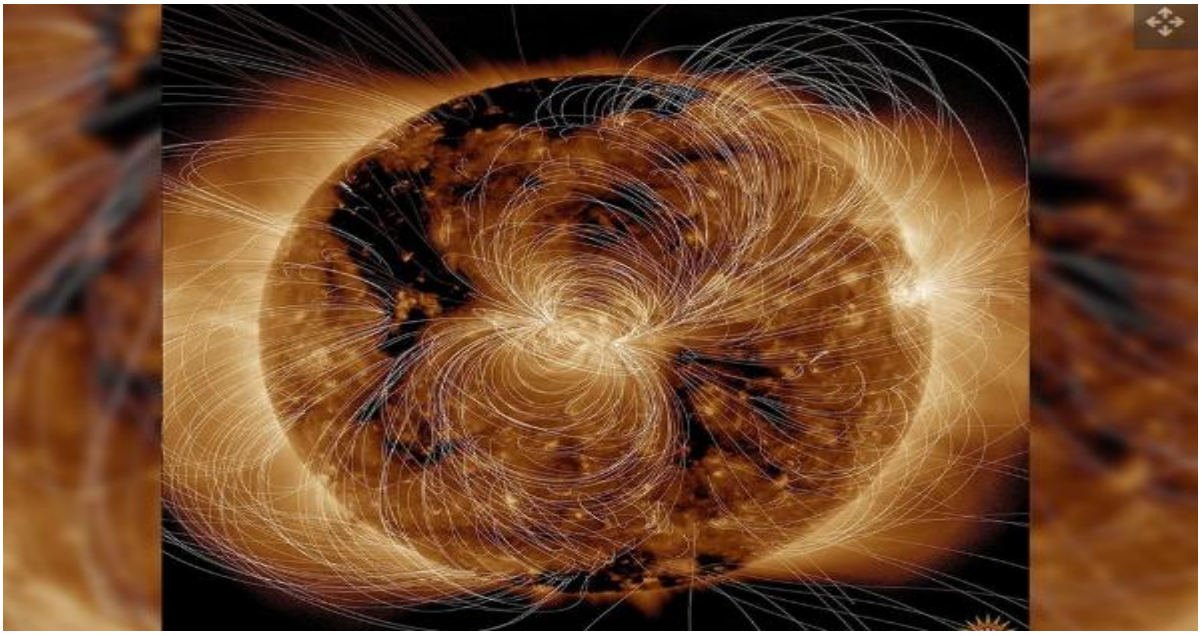

Figure 13: represents a depiction of the sun's magnetic field on its surface, looks like an human eye (adopted from ref [47]. Credit: NASA)

5.8 The First Cry of a baby star

Using the Chandra X-ray Observatory astronomers (CXO [48]) are able to capture the image of powerful x-ray emission from the plasma of the proto-stars those are passing through their neonatal phases. Analysis of their observed x-ray flare data (figure 14) hints that;

(a) The youngest neonatal phased star is hotter and 100-100, 000 times than the flare on our sun.
(b) This phase arises long before the maturity of their nuclear furnaces of hydrogen ignition getting maturity.
(c) These baby stars are appeared as firmly embedded in their cradle and crying much more tumultuously than expected.
(d) Special attention drawn to the astronomers by two youngest types of proto-stars: class 0 (zero) proto-star about 10, 000 years old (in human terms these proto-stars are like on hour old baby) and class 1 proto-stars of aged ~ 100, 000 years old (i.e. In terms of human ~ 10 hours old baby).
(e) Transition from one class to another class can be realized through the diminishes of the gas and dust-envelope in their infrared spectrum but all the most extreme activities are remained hidden until embedment in dense envelopes.

Significance is that analysis of the detected x-rays from 17 class 1 protostars located in the rho Ophiuchi molecular cloud 500 light years away from earth exhibit such type of "crying "similar to that of human baby [49]. This implies that stars make quite a fuss within their first days after birth, just like that observed in human babies on the earth.

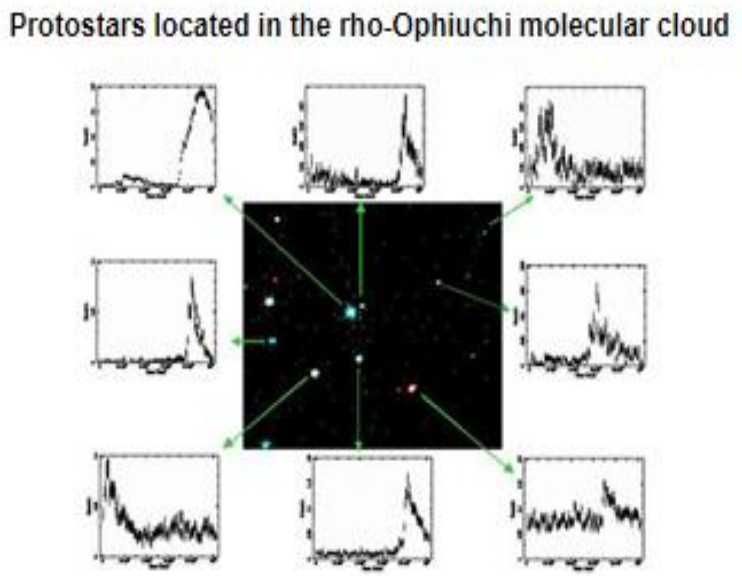

Figure 14: Schematic diagram showing 1 square light years field X-ray image around rho Ophiuchi molecular cloud core. Note: Red color represents less absorbed X rays, while blue represents absorbed X rays. Light curves for each source are also shown. (adopted from ref. CXO [48])

5.9 Sneezes of baby stars

In searching how baby stars develop astronomers recently capture the secrets of their infancy through ALMA radio-telescope by observing the proto-stellar disk that surrounds a baby star. Analysis of their observed data indicates an amazing fact that the baby stars discharge plumes of dust, gas and electromagnetic energy. Astronomers describe release of these magnetic flux as “sneeze” within the proto-stellar disk that is an essential part of star formation. This is similar in the case of human baby when taking first breath after delivery because of its surrounded air is full dust particles.

In fact, all stars develop from stellar nurseries which is full of large concentration of gas and dust that eventually take an important role to form a stellar core of a baby star through condensation. Thus, during the formation process gas and dust create a ring (called the proto-stellar disk) around the baby star.

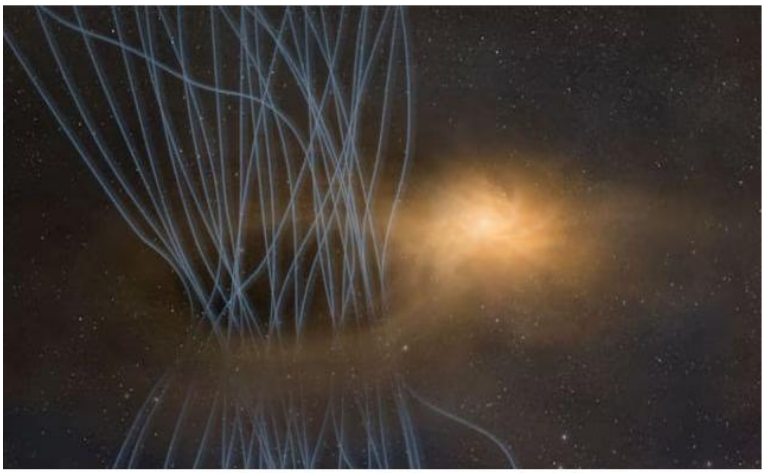

Figure 14: Illustrates an infant star "sneezing" out its magnetic flux. (Adopted from ref Kyushu University [50]. CREDIT: Kyushu University)

Magnetic field inside the core are able to penetrate perpetually this disk structure. As per observationally measured magnetic flux of known proto-stars astronomers suggested that there is a mechanism which is effective during the development of the star that remove the magnetic flux. This magnetic flux turns into “spike-like” structures extending a few astronomical units from the proto-stellar disk. The similar type of spike-like structures has been observed by astronomers during the other young baby stars. This implies that knowing the conditions that lead to the origin of these “sneezes” ultimately help us towards understanding of how stars and planets are formed i.e. what are complex processes involved in star formation.

6.Significance of this study

In the above it is seen that few characteristics of human baby are similar type with that of star’s baby. In other words, it can be said that the origin of such characteristics observed in stellar babies may provide us clues applicable to search or finding the origin of the characteristic in human baby. Two such important applications are related to: new insights in the human evolution and in the cosmic evolution.

6.1 New insights in the Cosmic Evolution

Cosmic Baby, Triaxiality and possible clue on the origin of motion in space time;

The NANOGrav 15-year data set study, based on the observations and timings of 68 old millisecond pulsars shows that motion in space-time i.e. evidence of the presence of low frequency gravitational wave background. Possible physical processes responsible for the origin of such low frequency gravitational wave are:

(a) Due to the signal coming from a population of supermassive black hole binaries (SMBH) located throughout the universe;
(b) Pulsars’ timing arrays (PTA) of 68 millisecond pulsars that are capable to produce nano-hertz frequency gravitational waves.

Discovery of cosmic baby provides us important information i.e.

i) The triaxial phase of a magnetar (i.e. neutron star) at birth time is strong enough to produce powerful gravitational waves with large amplitude;

In an investigation of millisecond pulsars with their emission of gravitational waves Chen [51] showed that the spin frequencies and their distribution of radio millisecond pulsars are the ideal source for continuous gravitational wave emission if the ellipticies >~ 10^{-9} and amplitude of characteristic strain h_o ~ (1.2-13.5) x 10^{-31}. In the present work I check ellipticity, characteristic age and "h_o" of the 68 millisecond pulsars considered in the NANOGrav observation (table I) and 40 young millisecond pulsars (table II) from out of 2000 pulsars data (de Araujo et al.2017 [52]) available in pulsar catalog and found.

A) in 68 millisecond pulsars
ellipticity (ϵ) of majority of the pulsars is ~ $10^{-18;}$
characteristic age (τ_c) ~ (1-10) G year;
amplitude (h_o) ~ 10-$^{37.}$
B) in 40 young millisecond pulsars
ellipticity (ϵ) of majority of the pulsars is ~ $10^{-8,}$ few have ~ $10^{-7;}$
characteristic age (τ_c) of majority (i.e. 30 out of 40 pulsars) is ranging (1-440) kyear
amplitude (h_o) ~ 10^{-32}-$10^{-33.}$

In brief, NANOGrav considered millisecond pulsars have characteristic age ~ G. year (i.e. Giga years) and the corresponding amplitude h_o is ~ 10^{-37} and ellipticity ~ 10^{-18} which are very much low in comparison to young millisecond pulsars with their characteristic age ~ k. year (i.e. kilo year), h_o ~ 10^{-32}-10^{-33}, and ellipticity ~ 10^{-8}.

Table 1: Parameters of 68 pulsars considered in NANOGrav Experiment

Pulsar	Period P (ms)	dP/dt (10^{-20}) s s^{-1}	Magnetic Field B_s x 10^{-8} G	Ellipticity (ϵ)	Characteristic Age (G. yr)	Amplitude h_o
J0023-0923	3.05	1.14	1.8869	--------	4.2418	---------
J0030+0451	4.87	1.02	2.255	2.183233 x 10^{-18}	7.5699	1.30 x 10^{-36}
J0340+4130	3.30	0.70	1.538	--------	7.4745	-----
J0406+3039	2.61	0.83	1.489	---------	4.9857	----------
J0437-4715	5.76	5.73	5.8135	1.45144 x 10^{-17}	1.5938	1.158 x 10^{-35}
J0509+0856	4.06	0.44	1.3525	----------	14.6298	---------
J0557+1551	2.56	0.72	1.3738	8.26608 x 10^{-19}	5.637	9.473 x 10^{-38}
J0605+3757	2.73	0.47	1.1462	---------	9.209	----------
J0610-2100	3.86	1.23	2.20	2.106686 x 10^{-18}	4.975	1.059 x 10^{-37}
J0613-0200	3.06	0.96	1.734	1.2921 x 10^{-18}	5.05378	5.348 x 10^{-37}
J0614-3329	3.15	1.74	2.369	2.42493 x 10^{-18}	2.870	1.014 x 10^{-36}
J0636+5128	2.87	0.34	0.999	4.26677x 10^{-19}	13.383	1.09 x 10^{-36}
J0645+5158	8.85	0.49	2.107	1.91646 x 10^{-18}	28.627	1.3433 x 10^{-37}
J0709+0458	34.43	38.02	36.612	---------	1.4357	------
J0740+6620	2.89	1.22	1.90	-------	3.7558	------
J0931-1902	4.64	0.36	1.3078	8.346415 x 10^{-19}	20.435	4.5216 x 10^{-38}
J1012+5307	5.26	1.71	2.1	3.95457 x 10^{-18}	4.877	8.649 x 10^{-37}
J1012-4235	3.10	0.66	1.4474	----------	7.447	-------
J1022+1001	16.45	4.33	8.54	3.13473 x 10^{-17}	6.023	6.619 x 10^{-37}
J1024-0719	5.16	1.86	3.1349	4.20145 x 10^{-18}	4.398	6.06 x 10^{-37}
J1125+7819	4.20	0.69	1.7226	--------	9.65	-------
J1312+0051	4.23	1.75	2.753	----------	3.832	-------
J1453+1902	5.79	1.17	2.633	2.9559 x 10^{-18}	7.846	3.92 x 10^{-37}
J1455-3330	7.99	2.43	4.458	8.53886 x 10^{-18}	5.213	7.65 x 10^{-37}
J1600-3053	3.60	0.95	1.871	1.50383 x 10^{-18}	6.008	2.73 x 10^{-37}
J1614-2230	3.15	0.96	1.759	1.33383 x 10^{-18}	90.057	8.117 x 10^{-37}
J1630+3734	3.32	1.07	1.9072	----------	4.919	----------
J1640 2224	3.16	0.28	0.9518	3.93822 x 10^{-19}	17.893	1.14 x 10^{-37}
J1643-1224	4.62	1.85	2.958	3.76270 x 10^{-18}	3.959	1.006 x 10^{-36}
J1705-1903	2.48	2.15	2.336	---------	1.828	--------
J1713+0747	4.57	0.85	1.994	1.71514 x 10^{-18}	8.524	2.94 x 10^{-37}
J1719-1438	5.79	0.80	2.1778	2.04833 x 10^{-18}	11.475	1.576 x 10^{-37}
J1730-2304	8.12	2.02	4.098	7.21938 x 10^{-18}	6.373	4.76 x 10^{-37}
J1738+0333	5.85	2.41	3.799	6.20297 x 10^{-18}	3.848	5.215 x 10^{-37}
J1741+1351	3.75	3.02	3.405	4.97851 x 10^{-18}	1.968	1.389 x 10^{-36}
J1744-1134	4.07	0.89	1.9259	1.61957 x 10^{-18}	7.25	1.019 x 10^{-36}
J1745+1017	2.65	0.26	0.839	3.185664 x 10^{-19}	10.159	1.406 x 10^{-37}
J1747-4036	1.65	1.31	1.4877	9.48855x 10^{-19}	2.012	2.549 x 10^{-37}
J1751-2857	3.91	1.12	2.1176	1.94670 x 10^{-18}	5.535	3.73 x 10^{-37}
J1802-2124	12.65	7.29	9.717	4.040173 x 10^{-17}	2.751	3.208 x 10^{-37}
J1811-2405	2.66	1.34	1.91	1.5689 x 10^{-18}	3.147	5.51 x 10^{-37}
J1832-0836	2.72	0.83	1.5204	1.031335 x 10^{-18}	5.1958	4.21 x 10^{-37}
J1843-1113	1.85	0.96	1.3485	7.7893 x 10^{-19}	3.055	4.90 x 10^{-37}
J1853+1303	4.09	0.87	1.9088	1.5700 x 10^{-18}	7.452	2.17 x 10^{-37}
B1855+09	5.36	1.74	3.09	----------	4.884	------

J1903+0327	2.15	1.88	2.0344	1.7781×10^{-18}	8.139	2.52×10^{-37}
J1909-3744	2.95	1.40	2.056	1.8155×10^{-18}	3.34	7.755×10^{-37}
J1910+1256	4.98	0.97	2.224	2.0295×10^{-18}	8.139	1.85×10^{-37}
J1911+1347	4.63	1.69	2.8306	3.48096×10^{-18}	4.343	4.3×10^{-37}
J1918-0642	7.665	2.57	4.4913	8.6457×10^{-18}	4.728	6.87×10^{-37}
J1923+2515	3.79	0.96	1.9302	1.5700×10^{-18}	6.259	4.67×10^{-37}
B1937+21	1.56	10.51	4.0974	------	0.2353	------
J1944+0907	5.19	1.73	3.032	3.901216×10^{-18}	4.7565	4.79×10^{-37}
J1946+3417	3.17	0.31	1.003	5.16059×10^{-19}	16.243	3.3891×10^{-38}
B1963+29	6.13	2.97	4.3177	------	3.2724	-------
J2010-1323	5.22	0.48	1.6017	1.10764×10^{-18}	17.242	1.38×10^{-37}
J2017+0603	2.90	0.80	1.5413	1.0575×10^{-18}	5.747	4.041×10^{-37}
J2033+1734	5.95	1.12	2.61	2.90536×10^{-18}	8.422	2.53×10^{-37}
J2043+1711	2.38	0.52	1.1257	5.48782×10^{-19}	7.256	3.277×10^{-37}
J2124-3358	4.91	2.06	3.218	4.46992×10^{-18}	3.779	1.896×10^{-36}
J2145-0750	16.05	2.98	6.998	2.13402×10^{-17}	8.539	6.515×10^{-37}
J2214+3000	3.12	1.47	2.167	1.92132×10^{-18}	3.365	8.354×10^{-37}
J2229+2643	2.98	0.15	0.676	1.91293×10^{-19}	31.496	6.38×10^{-38}
J2234+0611	3.58	1.20	2.0974	--------	4.73	---------
J2234+0944	3.63	2.01	2.7333	----------	2.863	--------
J2302+4442	5.19	1.39	2.7179	3.03808×10^{-18}	5.919	6.356×10^{-37}
J2317+1439	3.45	0.24	0.920	3.66859×10^{-19}	22.791	6.918×10^{-37}
J2322+2057	4.81	0.97	2.1857	2.05210×10^{-18}	7.8621	4.81×10^{-37}

Table 2: Parameters of young pulsars with Kyr ages

Pulsar	**Period P (s)**	**dP/dt (10^{-12} s. s^{-1})**	**Magnetic Field B_s x 10^{-13} G**	**Ellipticity (ϵ)**	**Charact-Triaxial phase con-eristic tinues for next Age period k. yr k yr Inference ***	**Value of h_o**
J0100-7211	8.02039	18.80	3.929	6.6345×10^{-6}	6.763 993.3 kyr **Not Triaxial Star**	7.308×10^{-33}
J0146+6145	8.68899	1.99022	13.304	7.608×10^{-7}	69.2 930.8 kyr Triaxial Star	1.184×10^{-32}
J0157+6212	2.35175	0.18901	6.667	1.955×10^{-8}	197.36 803 kyr Triaxial star	9.289×10^{-33}
J0501+4516	5.7621	5.8196	18.5306	1.475×10^{-8}	15.69 984.3 kyr **crossed**	8.544×10^{-32}
J0534-6703	1.81757	0.42501	2.825	3.398×10^{-8}	67.8 932 kyr Triaxial star	8.755×10^{-34}
J0720-3125	8.39112	0.0698	2.449	2.577×10^{-8}	1905.84 **crossed**	3.870×10^{-33}
J0726-2612	3.44231	0.29302	3.2138	4.437×10^{-8}	186 814kyr Triaxial star	5.263×10^{-33}
J9847-4316	5.97749	0.1200	2.71	3.156×10^{-8}	790 210 kyr Triaxial star	2.780×10^{-34}
J1001-5939	7.73364	0.05989	2.177	2.038×10^{-8}	2047 **crossed**	4.368×10^{-34}
J1022-5813	1.64373	0.14501	1.562	1.048×10^{-8}	180 820kyr Triaxial star	5.472×10^{-34}
J1050-5953	6.45208	0.38978	5.017	1.081×10^{-8}	2.68 997 kyr Triaxial star	1.221×10^{-31}
J1107-6143	1.7994	0.15599	1.695	1.235×10^{-8}	183 817kyr Triaxial star	1.176×10^{-33}
J1119-6127	0.40796	4.01975	5.2476	7.216×10^{-8}	1.6 998.4kyr Triaxial star	2.183×10^{-31}
J1513-5908	0.151251	1.5300	0.7405	1.018×10^{-8}	1.56 998.5kyr Triaxial star	4.275×10^{-31}
J1524-5706	1.11605	0.3559	2.0169	1.748×10^{-8}	50 950 kyr Triaxial star	2.749×10^{-33}
J1622-4950	4.3261	16.99	27.440	9.491×10^{-6}	4 996 kyr Triaxial star	8.002×10^{-32}
J1632-4818	0.813453	0.64998	7.358	2.326×10^{-8}	20 980 kyr Triaxial star	1.741×10^{-32}
J1708-4008	11.0063	0.01960	2.3978	9.4918×10^{-6}	8.9 991 kyr **Not Triaxial star**	8.721×10^{-32}
J1714-3810	3.82494	0.58803	5.176	9.895×10^{-6}	1 999 kyr **Not Triaxial star**	2.167×10^{-31}
J1718-3718	3.37857	1.6099	7.485	2.393×10^{-7}	33.2 966.8 kyr Triaxial star	1.745×10^{-32}
J1726-3530	1.11013	1.2201	3.7242	5.959×10^{-8}	14.4 985.6kyr Triaxial star	2.051×10^{-32}
J1734-3333	1.16934	2.2798	5.2457	1.173×10^{-7}	8.1 992 kyr Triaxial star	4.904×10^{-32}
J1740-3015	0.606887	0.4660	1.7017	1.244×10^{-8}	20.7 979.3kyr Triaxial star	3.572×10^{-31}
J1743-3150	2.41458	0.1210	1.7296	1.285×10^{-8}	316.4 783.6kyr Triaxial star	2.556×10^{-33}
J1745-2900	3.76373	0.17599	26.043	2.914×10^{-6}	3.39 996. kyr **Not Triaxial star**	1.048×10^{-31}
J1746-2850	1.0771	1.3399	3.8443	6.350×10^{-8}	12.74 987.2kyr Triaxial star	1.8×10^{-32}
J1808-2024	7.55592	548.997	206.100	1.825×10^{-4}	21.82 978.2 kyr **Not Triaxial star**	1.040×10^{-30}
J1809-1943	5.54035	7.7696	20.995	1.895×10^{-6}	11.3 988.7kyr **Not Triaxial star**	7.251×10^{-32}
J1819-1458	4.26316	0.5750	5.0101	1.078×10^{-7}	117.5 882.5kyr Triaxial star	6.588×10^{-33}
J1821-1419	1.65601	0.8949	3.8956	6.521×10^{-8}	29.3 970.7kyr Triaxial star	8.431×10^{-33}
J1830-1135	6.22155	0.04769	1.7432	1.3057×10^{-8}	2068.4kyr **crossed**	3.272×10^{-34}
J1846-0287	4.47672	0.1609	2.7166	3.171×10^{-8}	440.8 559.2kyr Triaxial star	1.427×10^{-33}
J1846-0258	0.32657	7.1104	1.5420	1.021×10^{-7}	0.72 999.3kyr Triaxial star	6.987×10^{-31}
J1847-0130	6.70705	1.2699	9.3393	3.747×10^{-7}	83.7 916.3kyr Triaxial star	4.612×10^{-33}

J1854-0306	4.55782	0.14501	8.2267	2.907×10^{-8}	498.3 502.7kyr Triaxial star	2.479×10^{-37}
J1855+0527	1.39348	0.26699	6.1723	1.637×10^{-8}	82.75 917.3kyr Triaxial star	3.676×10^{-33}
J1901+0413	2.66308	0.1320	1.8973	1.546×10^{-8}	319.9 780.1kyr Triaxial star	1.335×10^{-33}
J1918+1444	1.18102	0.21198	1.60112	1.1016×10^{-8}	88.3 911.7kyr Triaxial star	2.639×10^{-32}
J1924+1631	2.93519	0.36399	3.3076	4.7009×10^{-8}	12.78 987.2kyr Triaxial star	8.141×10^{-34}
J1941+2525	2.30615	0.16099	1.94981	1.6336×10^{-8}	227.2 772.9kyr Triaxial star	8.46×10^{-34}

This means that the characteristic strain i.e. motion produced in space-time is effectively more when these 68 millisecond pulsars were with their characteristic age ~ k. year rather than ~ G. year. This implies that these 68 millisecond pulsars were possessing the ellipticities within the range 10^{-7}-$10^{-8.}$ Chau et al [53] showed that millisecond pulsars passing through their triaxial phases for a period of ~ 10^{6} years with the ellipticities ranging ~ 10^{-7} to $10^{-8i.e.}$ millisecond pulsars, having ellipticities ~ 10^{-7}-10^{-8}, exhibit their triaxial nature for a period of ~ 10^{6} years. In the case of NANOGrav 68 millisecond pulsars one can assume the real fact nano-hertz gravitational background was created when they had been exhibiting their triaxial nature during their characteristic age ~ $\leq 10^{6}$ years and ellipticities ~ 10^{-7}-$10^{-8.}$ Thus, the author suggests these 68 millisecond pulsars were "Triaxial Stars" in nature so that they are capable of producing low frequency gravitational waves in space-time.

6.2 Hourglass structure / shape in Cosmic Development

Hourglass shapes or structures have been observed in cosmic environment ranging from supernova explosion (i.e. star formation to star's death) to magnetic field evolution. Core collapse supernovae (CCSNe) offer the astronomers/ scientists a unique opportunity to investigate (i) the last stages of stellar life, cycles, (ii) the synthesis of heavy elements synthesis and (iii) the origin or birth of compact objects. Not only that, facts like generation of interacting stellar winds for the production of non-spherical planetary nebula (PNe) involving a strong equatorial density enhancement in red giant, in white dwarf; extremely elongated nebulae, and bipolar shells with very narrow waists are also faced through Hourglass shapes. So, underlying physics of explosion mechanism and electromagnetic signal emitted from the environment of compact objects, jets from the envelopes, etc. can be considered as a probe to study the Hourglass shapes in various cosmic phases. Few observed hourglass shapes in various studies, investigations are mentioned below:

(i) Hourglass shape in SN1987A

During the study of supernova SN1987 Burderi and King [54] found a complex three ring shaped structure that extends some arc second around the central spot of SN1987A. On thorough analysis they found such structure has arisen due to the fact when a thin shell of matter surrounding the supernova was illuminated by ignition extreme-UV flash produced from the explosion of the progenitor. They also found a bright Hourglass shaped nebula surrounding the supernova as well as a small central ring that is located at the waist of Hourglass. This was the first visible to the naked eyes after the Kepler's supernova of 1604.

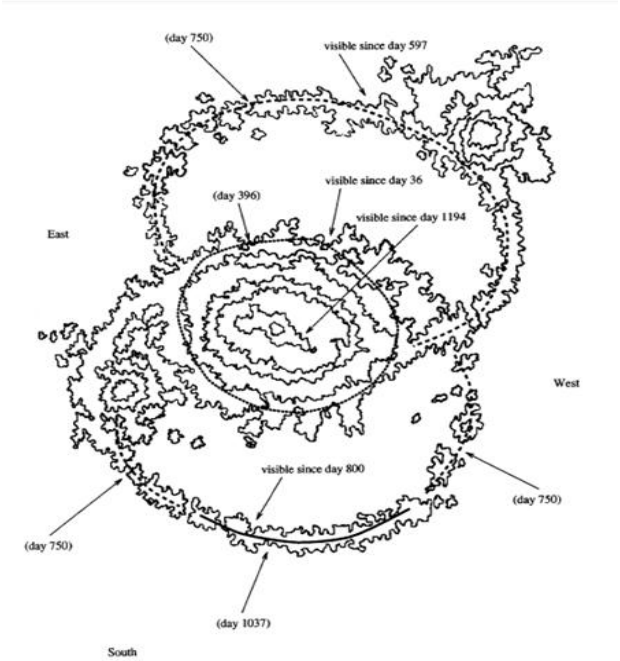

Figure 15: shows the sketch of the HST image of the SN1987A taken in February 1994. The dotted line indicates the inner ring structure (with the northern rim of the nearer outer ring overlapped) first seen at ESO; the dashed lines indicate parts of the outer rings first seen at Las Campanas Observatory (adopted from ref. [54])

Figure 15 (a) shows the image of the Supernova SN1987A captured by Hubble space telescope (HST) in January 2017. This new image of the supernova provides clues to the scientists / astronomers for a better standing of these cosmic explosions. (Credit: NASA).

(ii) Hourglass shape in young planetary nebula MyCn18

Figure 16: Sahai et al [55] obtained composite color image of MyCn18 showing Ha (green), [N II] (red), and [O III] (blue) emission (the color balance has been adjusted such that regions where the [N II] and Ha overlap appear orange). The image covers an area (540 24A.59] 23A.32] 512 pixels).

Figure 16 shows an Hourglass shaped image of young planetary nebula MyCn18 located ~ 8000 light years away from us. Sahai et al [55] observed it with the help of Wide Field and Planetary Camera 2 (WFPC2) on board NASA's Hubble Space Telescope (HST). It reveals from the analysis of HST observed data that the true shape of MyCn18 to be an Hourglass. The significance of this observed shape is that it lights on the poorly understood ejection of stellar matter which accompanies the slow death of star. They suggested that this Hourglass shape is produced by a fast stellar wind within a slowly expanding dense cloud located near the equator.

(iii) Hourglass shape observed in star forming region Lagoon Nebula M8

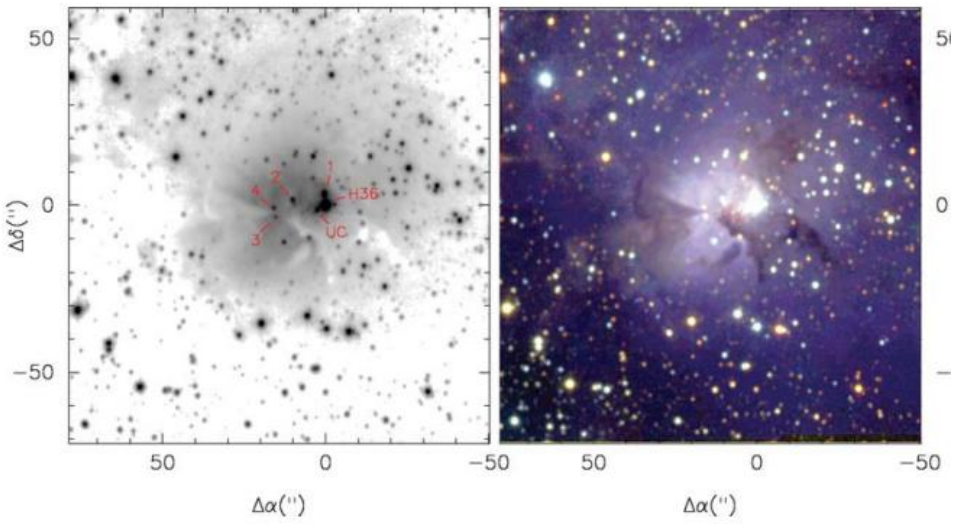

Figure 17: shows (Left-hand panel): Ks image of the field surrounding the Hourglass nebula as observed by Arias et al [56]. Labelling: the ionizing O7.5 V star Her 36 (H36), the infrared sources KS 1-KS 4 and the ultracompact H II region G5.97-1.17 (UC). The right-hand panel shows three-colour near-infrared image of the same field. Note that the large majority of sources in this image are not visible at optical wavelengths.

It is an extended H II region that is mainly ionized by two O-type stars and embedded within a molecular cloud extending to the star cluster NGC 6530 (i.e. NGC 6523-6530). In a study Arias et al [56] observed a distinctive Hourglass shaped bipolar nebula in that H II region (Figure 17). Analysis of the observed data suggests that this Hourglass is believed to be an ionized cavity having inhomogeneous clumpy molecular cloud. This Hourglass shaped region also harbours an ultracompact H II region with a number of infra-red sources as observed through HST observation. However, New Technology Telescope through long slit spectrum confirms.

(a) The identification of HH870 in the core of the Hourglass nebula, and
(b) The first direct evidence of active star formation by accretion in M8.

(iv) Hourglass shape in Protostar L1527

Figure 18: Hourglass shape in the proto-star L1527 as captured by JWST (Courtesy: NASA)

Recently, James Webb Space Telescope (JWST) captured a spectacular hourglass image formed in an embedded growing situation when a cloud of material is feeding. Note that ejected material of the star form cavities above and below it. The blue and orange clouds in the image outline cavities created as material shoots away from the protostar and collides with the surrounding matter. Significance is that;

a. The protostar doesn't yet generate its own energy through nuclear fusion of hydrogen, yet it indicates an essential characteristic of stars.
b. Its shape-a puffy clump of hot gas somewhere between 20% and 40% of the mass of our sun-is also unstable.
c. The image provides context for historical background i.e. What our sun and solar system looked like in their infancy.

(v) Hourglass shape in Isolated Pulsar PSR B1828-11

During an investigation of the spin dynamics through comparative analysis of the predicted spin dynamics with the observed pulse duration Link and Epstein [57] fond a nonstandard hourglass shape (Figure 18).

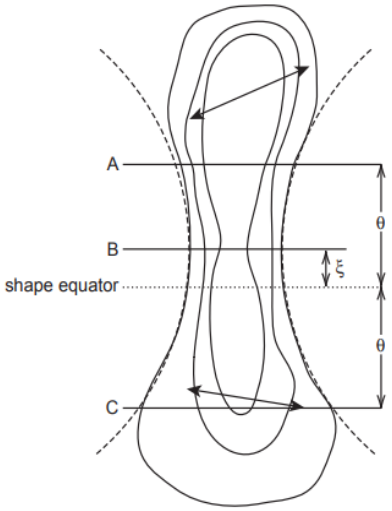

Figure 19-The beam pattern as observed by Link and Epstein [57] for the radio emission from PSR B1828-11. The dashed parabolas represent the analytic fit to the beam width, and the contour curves are one possible realization of the actual beam shape. As the star precesses, observer's line of sight varies by ±θ about the star's shape equator, the dotted horizontal line. The solid lines A and C give the range of the viewing angles. Line B represents the viewing angle at which the beam is the narrowest. The double-headed arrows represent plausible polarization directions (adopted from ref [57])

(vi) Hourglass shape in Magnetar

Recently, Hurley-Walker et al [58] discover a new type magnetar with a long period (21min) radio transient (now known as GPM J1839-10). It's radio pulse brightness varies between 30-300s and have a quasi-periodic substructure. Scientists of International Centre for Radio Astronomy Research (ICRAR) have performed simulation study of such magnetar and found an hourglass structure as shown in figure 19. Significance of this discovery is that it will help for understanding the physics of neutron stars and the behavior of magnetic field in extreme environments.

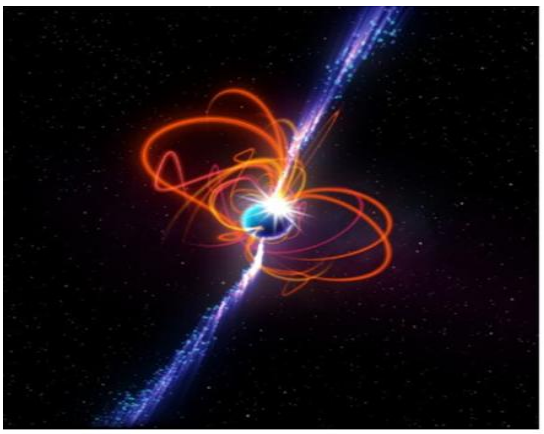

Figure 19: shows an artist's impression of a magnetar having ultra-strong magnetic field that can produce such powerful bursts of energy (Credit: ICRAR)

(vii) Hourglass shape observed in Magnetic field

G240.31+0.07 is an active high mass, star forming region having a bolometric luminosity of

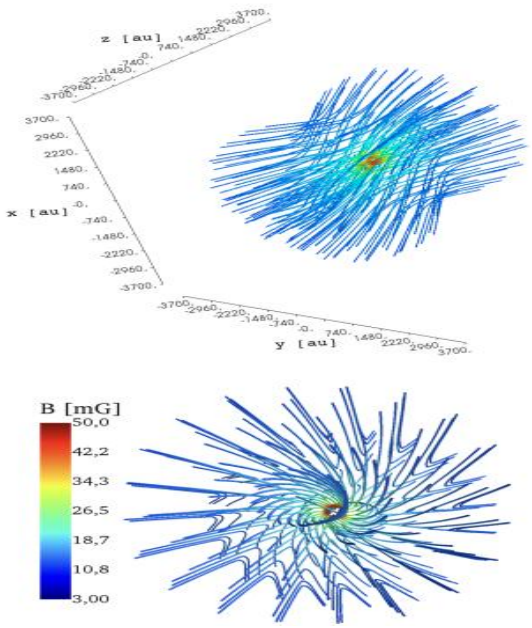

Figure 20: shows the observed hourglass structure in simulation study. Upper panel: magnetic field configuration inside a radius of 3700 au, corresponding to the radius of the Main core in G31, for b0 = 0.1, i = −45◦, and ϕ = −44◦. Lower panel: magnetic field line configuration for b0 = 0.1 shown almost pole-on to emphasize the line twisting close to the symmetry axis. The spatial scale is the same in both panels (the model extends up to a radius of 3700 au). The color of the magnetic field lines indicates the magnetic field strength in both panels. (adopted from ref [59])

10^{45} L_o at a distance of 5.32 kpc. Qiu et al [59] observed the polarized dust emission at 0.88mm through the sub-millimeter array and found a clear hourglass shaped magnetic field aligned within 20^0 of the outflow axis (Figure 20). Significance of this observation hints that both the magnetic field and kinematic properties observed in this region are surprisingly consistent with theoretical predictions regarding the paradigm of isolated high mass star formation.

(viii) Hourglass shape observed in Magnetic field in Class 0 Protostar L1157-mm

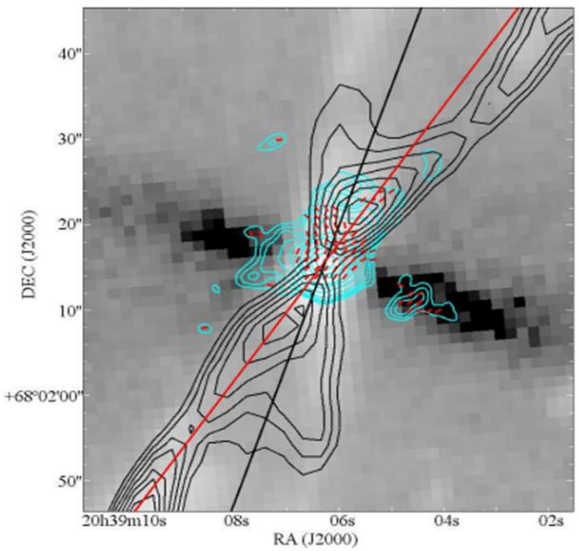

Figure 21: shows the Hourglass morphology of L1157 with the axis of the hourglass (red line) and the center of the outflow (black line) as obtained by Stephens et al [60].

Stephen et al [60] first detected the polarization around the polarization around the Class 0 low-mass protostar L1157-mm at two different wavelengths. This polarimetric map show inferred magnetic field lines aligned with the outflow. This observation suggests a full hourglass magnetic field morphology centered about the core; this is only the second well-defined hourglass detected around a low-mass protostar to date.

(ix) Hourglass shaped Planetary Nebula Hubble 12

In an investigation on planetary nebula Hubble 12, using optical imaging and long slit spectroscopy, Vaytet et al [61] found first time the presence of end caps or knots which is aligned with the bipolar lobes of the planetary nebula shell of Hb 12 (Figure 22). Precise estimation shows the inclination angle of the Hourglass-shaped nebula is ~ 60^0 to the line of sight. Vaytet et al also suggested that central star system of Hb12 may be an eclipsing binary which have high velocity "knots" (with Hubble type velocities) close to the core of Hb12. Calculated values of different velocities and kinematical ages indicate the origin of the outer and inner knots may be from different outburst events.

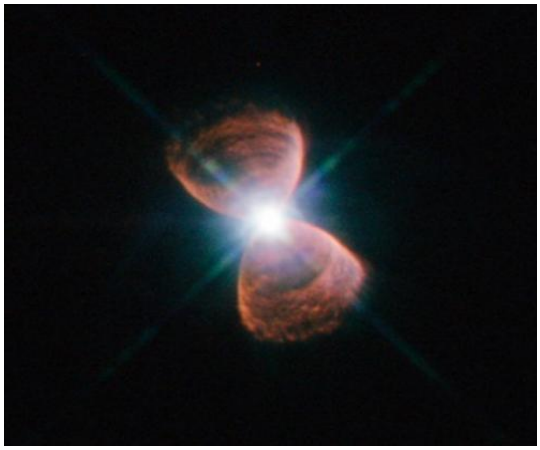

Figure 22: shows the image of Planetary Nebula Hb 12 taken with the NASA/ESA Hubble Space Telescope. This nebula (catalogued as PN G111.8-02.8) lies in the constellation of Cassiopeia. The striking shape of Hubble 12, reminiscent of a butterfly or an hourglass, was formed as a Sun-like star approached the end of its life and puffed its outer layers into the surrounding space. For bipolar nebulae, this material is funneled towards the poles of the ageing star, creating the distinctive double-lobed structure. (Adopted from ref [61].

(x) Hourglass shaped Cocoon inside a dying massive star

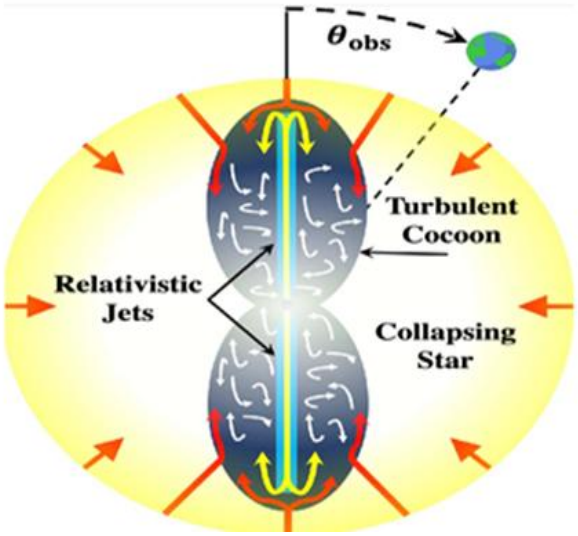

Figure 23: Schematic diagram showing jets (light blue) inflated Hourglass-shaped Cocoon (dark blue) inside a dying massive star (pale yellow). In this case jets run into and shock against the collapsing star that form a backflow (yellow arrows) while the in-falling star runs into and shocks against the backflows indicated by red arrows. White arrows indicate the mixing of the shocked jets and shocked stellar components that form the Cocoon and turbulent inside the star (adopted from ref [62])

The presence of intervening opaque stel lar gas creates constraint to the astronomers on understanding the underlying physics of supernova explosion mechanism and the realistic picture of compact object environment. The state-of-the art-based 3D general relativistic magneto-hydrodynamic simulations, performed by Gottlieb et al [62], show the dying massive star produces bipolar relativistic jets that inflate a turbulent energetic bubble into the form of "Cocoon" inside the star (Figure 23). Further investigations by Gottlieb et al show that these Cocoons emit quasi-isotropic gravitational wave ~ 10-100Hz (i.e. within the detectable range of LIGO-Virgo-KAGRA (LVK) detectors, band ~ 10-100Hz) over a characteristic jet activities time scale ~ 10-100 s. As the electromagnetic radiations are emitted from energetic core collapse supernovae and the

Cocoons, Gottlieb et al predict that these collapsars are powerful multi-messenger events that can be studied through the observations and analysis of the associated electromagnetic radiations.

(xi) Hourglass structure in Galaxy

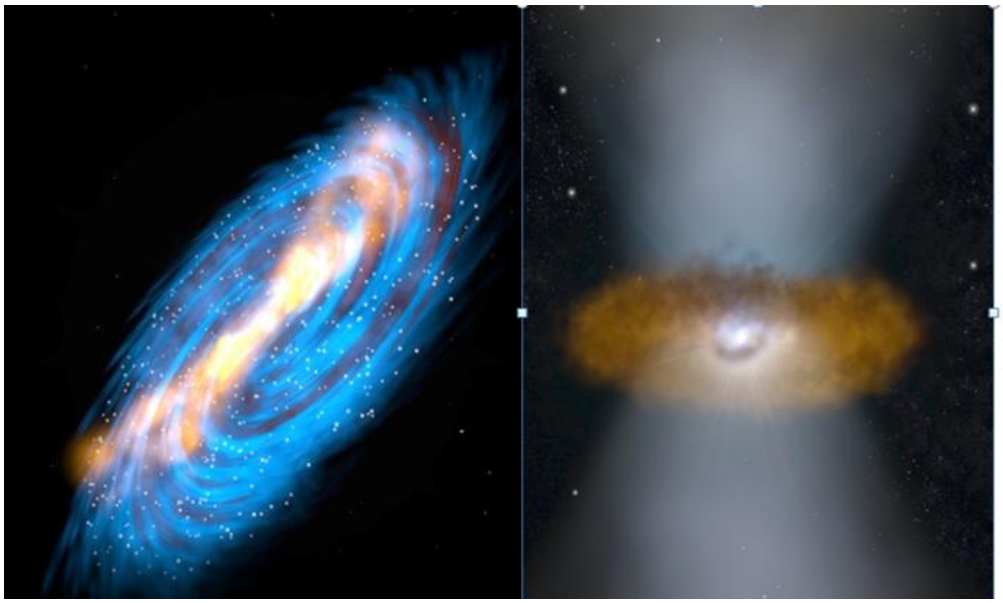

(A) **(B)**

Figure 24: shows Hourglass structure arises (A) as the gas in the galaxy's spiral arms interacts with light produced near the black hole at the center, affecting the gas flow (B) Markarian 573 is an active galaxy located about 240 million light-years away in the constellation Cetus (adopted from ref [63])

The Markarian 573 is an active galaxy located about 240 Mpc away from us. A supermassive black hole sits at the center of it sits a supermassive black hole that pulls matter towards it, and this material produces high-energy light as it's gobbled up. This light, however, is unable to escape as it is blocked by a dense ring of dust and gas surrounding the black hole. Light can only escape through cone-shaped areas above and below this ring. These cones of light give the galaxy's inner region its signature hourglass shape (Figure 24) as seen by NASA's Chandra X-ray Observatory [63]. Gas clouds orbiting around the galaxy become electrically charged when they pass through this powerful emission while those Gas less than 2, 500 light-years from the black hole accelerates away, forming fast-moving outflows. Farther off, the gas becomes charged but stays in the galaxy's disk. Significance of this discovery is that the "feedback process" may help scientists to understand why galaxies like Markarian 573 have such an odd structure and unusual gas motions.

(xii) Hourglass shape in dwarf galaxy

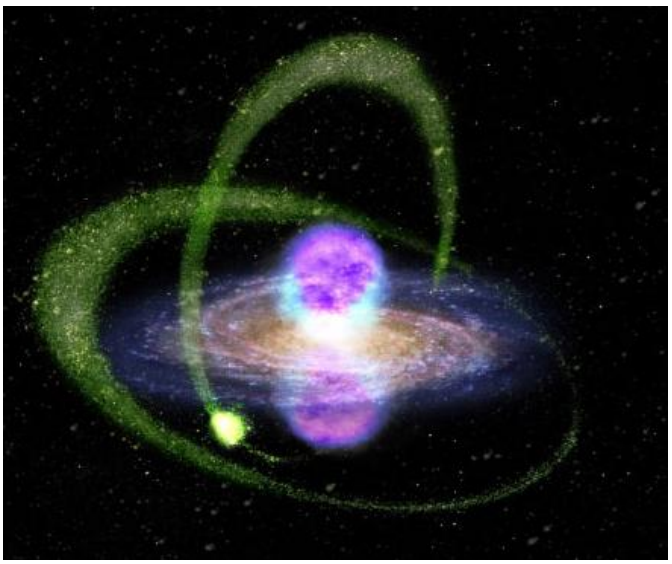

Figure 25: Crocker et al [64] observed Hourshaped structure in Sagittarius galaxy.

The Sagittarius dwarf spheroidal galaxy is an elliptical loop-shaped galaxy located ~ 78, 300 light-years away from us. In an investigation Crocker et al [64] focused on the Fermi bubble whose peculiar structure is clouds of gas towering about 30, 000

light years above and below the plane of our Milky Way galaxy. They observed significant gamma ray emission coming from a population of millisecond pulsars located within the galaxy and Hourshaped appearance arises due to the significant gamma ray emission coming from the millisecond pulsars populated within this galaxy.

(xiii) Hourglass structure in Galaxy due Black hole

In 2020, the X-ray satellite eROSITA captured image of two gigantic bubbles extending to 80^0 above and below the center of our own Milky Way galaxy (Figure 26). The morphology of these two bubbles shows a remarkable resemblance to the earlier observed bubbles by NASA's Fermi Gamma Ray Space Telescope and its counterpart. The main problem regarding the physical origin of these striking structures is still remain.

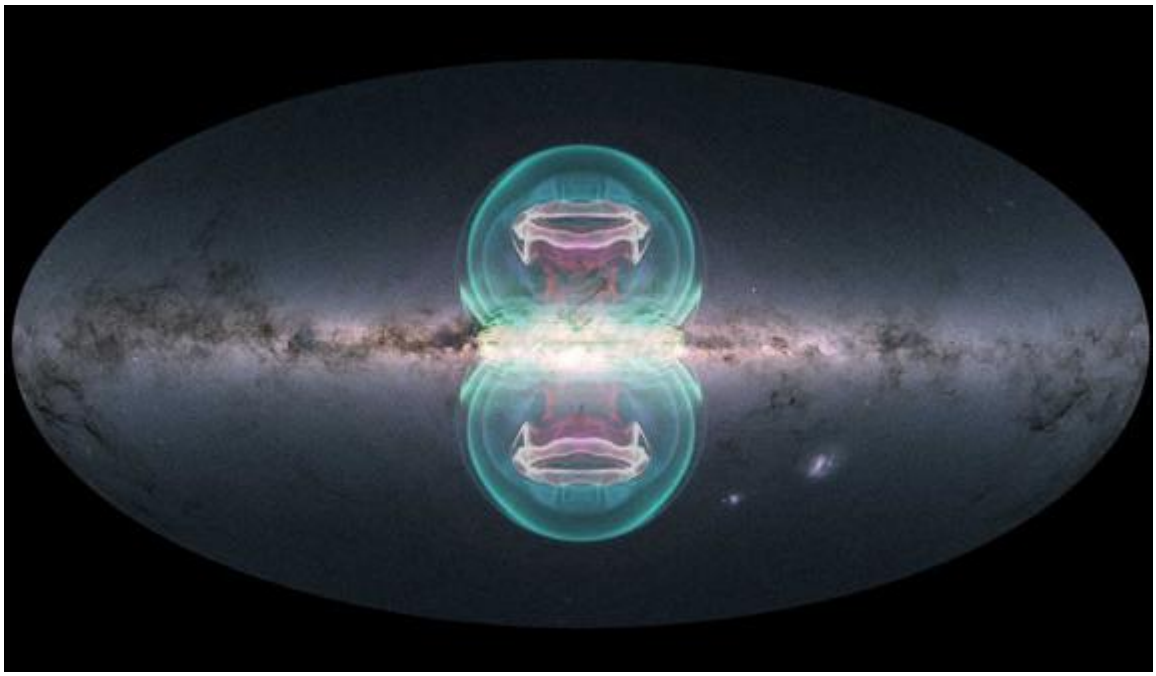

Figure 26: Yang et al [65] observed Hourglass shaped bubbles as relics of the past activity of the Galaxy's central black hole.

But based on this observation Yang et al [65] suggest that the origin is probably from some energetic outbursts from the Galactic center in the past. However, they propose a theoretical model explaining the origin probably due to a single event of jet activity from Sagittarius A^*-a supermassive black hole with mass 4.3 -million -solar mass black hole located at the center of Milky Way galaxy and that jet activities occurred ~ 2.6 million years ago and lasted about 100, 000 years.

The significance of these findings are it will help the astronomers to understand how black holes interact with the galaxies that they are inside, because this interaction allows these black holes to grow in a controlled fashion as opposed to grow uncontrollably.

(xiv) Variable stars follow Hourglass shape

Figure 27 shows the spectacular image of the planetary nebula CVMP1 (captured by International Gemini Space Observatory) located around 6500 light years away in the southern Constellation of Circinus. The main noticeable fact is that this image will fade from view over thousands of year as its progenitor star cools slowly. This CVMP1 emerged when an old red giant star blow off its outer layers in the form of a hotter stellar wind. As a result, astronomers have found the gases making up the hourglass are highly enriched with helium and nitrogen. Significance of this discovery is that it is highly evolved.

Figure 27: Spectacular image of the celestial containing planetary nebula CNMP1 (adopted from ref [66])

6.3 New insights in Human Development

A) Hourglass in female body shape

The Hourglass body shape is named primarily on the resemblance to that of an hourglass. The Hourglass figure is one of the four traditional female body-shapes: Rectangular (or scale shape), Apple or inverted triangle, Pears and Hourglass. The Hourglass shape in a woman's body is defined basically by the measurement-the circumference of the bust, waist and hips.

Hourglass body shapes have a wide bust, a narrow waist and wide hips with a similar measurement to that of the bust i.e. the upper and lower half are wide and roughly equal where the middle is narrow in circumference so that overall body shape presentation: wide-narrow-wide (figure 28).

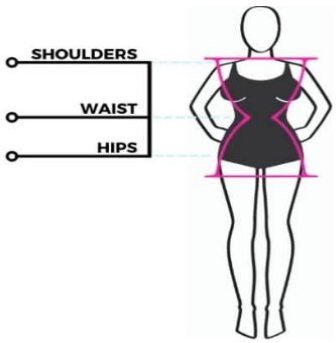

Figure 28: Schematic diagram showing the Hourglass shape in female body

Properties of woman's Hourglass figure.

Women who exhibit the Hourglass figure.

(i) Receive more admiration;
(ii) Possess "gynocoid" pelvis which is low and wide;
(iii) This shape is considered ideal for child birth. Women with such structure will be able to deliver a child more easily.
(iv) Scientists believe that female body shape is result of evolutionary adaptation for reproductive fitness. Reason is that it conveys information about gene quality, health and fertility.
(v) Women's such body shapes reflect the fact of adaptation to reproduction and locomotion i.e. during pregnancy their body is transformed means the center of gravity turns off balance. To prevent this off balance, it is believed that evolution could have flavored fat deposition in the gluteal region and the thighs [67].

(vi) Sex hormones can influence such body shape i.e. during fat accumulation to the abdominal region estrogen decreases that stimulate fat growth in the lower body.

B) Characteristic of Newly born human baby

After fertilization about 40 weeks are required for the birth of a new baby. During the stay of 40 weeks inside the mother's womb various changes, towards turning from an egg into full baby form, would occur that have been observed via ultrasonography (USG) images. Ultrasonography i.e. prenatal ultrasound checking, therefore, is the realistic picture or image on the health and development of the growing baby inside the mother's womb. In pregnancy the first 12 weeks is a very crucial time for fetal development. As per our present scientific conception, a zygote is formed from the combination of the egg and sperm. This zygote becomes an embryo through the progress of cell division and grows. Ultrasonography image (see figure 3A, B & Fig4. A, B) shows the first significant noticeable fact is the ellipsoidal shape of the Gestational Sac. Initially a gestational sac (or chorionic cavity) is located with a light paracentical position in the decidua. As per observational measured data it has a rapid growth ~ 1 mm per day. The clear picture of its borders, captured in USG image, when its size appears with mean diameter of 2-4 mm.

Analysis of the ultrasonography (USG) image of gestational sac at week 5 (approx.) shows that;

(a) The embryo is surrounded by a large cavity of fluid so called gestational sac;
(b) Its normal position is within the uterus;
(c) Ultrasonography images clearly show that its initial shape is circular but it becomes more ellipsoid with the appearance of the yolk and the embryo. This shows the physical evidence the gestational sac turns from its initial circular shape to more ellipsoid.

C) Woman's beautiful face with youthful energy and ageless presence

If we look surrounding us on can find ~ 10 % women whose faces are beautiful, ~ 1-2 % women having faces are so beautiful with youthful energy and age-less presence so that they are automatically attracted in our eyes. Even any one can easily distinguish them from rest of the others. The question naturally arises in our mind-"Why these women have very beautiful facial structure and also of body structure indicating full of energy and spontaneously exhibiting special appearance with age-less presence i.e. look like more younger comparatively than that would be w. r. t. their actual age.

Each human baby must pass through the zygote phase, the embryo formation phase and then gradual development phase. Thus, all women should be of almost same facial structure. But actually not (?). Why their appearances do not same as that of the others? Possibly, the secret lies in the triaxial phase i.e. when, how much deformation (i.e. triaxiality) during the change in shape of the gestational sac from circular to ellipsoidal shape. In relativistic case, compact object turns into triaxial star when its shape changes from Maclaurin spheroid to Jacobian ellipsoid due to increase in rotation. In the case of human baby Gestational Sac changes its shape from circular (i.e. spheroidal) to ellipsoidal shaped due to its growth under gravity. This means that triaxial phase appears during the period of turning from initial circular to ellipsoidal shape implying that triaxial phase of gestational sac, in particular gestational sac suffering from triaxial nature would have an important effect on embryo resulting which new baby possesses the characteristic of very beautiful face and body structure with youthful energy and ageless presence.

No doubt, triaxial phase of gestational sac at the initial stages plays an important role and moulding the embryo resulting which women possess beautiful faces after their birth but searching of what exact role / happenings need further investigation.

D) Cosmic Baby, Triaxiality and possible Origin of Human Beautiful Face, Age less appearance

Astronomers / scientists observed that human baby and star's baby both exhibit a similar type characteristics like "umbilical cord", "first cry", "sneeze", etc. Thus, origin of that characteristics in cosmic baby can be applicable to find the possible clues of similar characteristics observed in human baby, although the real situations are different from one another. In cosmic baby or star's baby relativistic gravity is active while in human baby normal gravity is effective. According to the theoretical work of Chandrasekhar (1969) on triaxial star shows that the classical solution of Maclaurin spheroids and Jacobian ellipsoids for a self-gravitating, uniformly rotating, incompressible fluids in equilibrium gives two possible situations i.e. when the rotation of an equilibrium configuration is increased then;

(a) The sequence of the axisymmetric Maclauring spheroids diverges to the sequence of triaxial Jacobian ellipsoids such that
(b) The ratio of kinetic (T) to gravitational (W) energy reaches $T/|W| \sim 0.14$ (Bonazzola et al [54]).

As a result, the configurations are no longer precise ellipsoidal in relativistic gravity or for compressible fluids the appearance of triaxially deformed rotating compact stars (i.e. simply Triaxial Star) which are rather than ellipsoids. This means that the

triaxial model is very important in relativistic astrophysics as well as this triaxial model is also applicable in human case where transformation from spheroidal to ellipsoidal arises.

E) Hourglass in Human mind

It is believed that human mind is like an hourglass structure with one half bulb within physical reality and another half out of it. Physically we observe few women having hourglass shape with ageless appearance also [68]. In general, 8-10 % women are with hourglass structure and ageless appearance. In searching of such structure Assadi [69] assumed human mind as a sand hour structure in which one half is associated with the cloud section representing the structure of physical reality while the other half is out of it (figure 29). Note that the bottom section represents the structure of mind. Our mind that is related to our consciousness as well as the part of mind through which interaction is made with the physical world. While another part of bulb shape structure is related to the non-physical world or out of space time continuum i.e. our known multidimensional reality. In this part mind containing the unconsciousness or non-physical component.

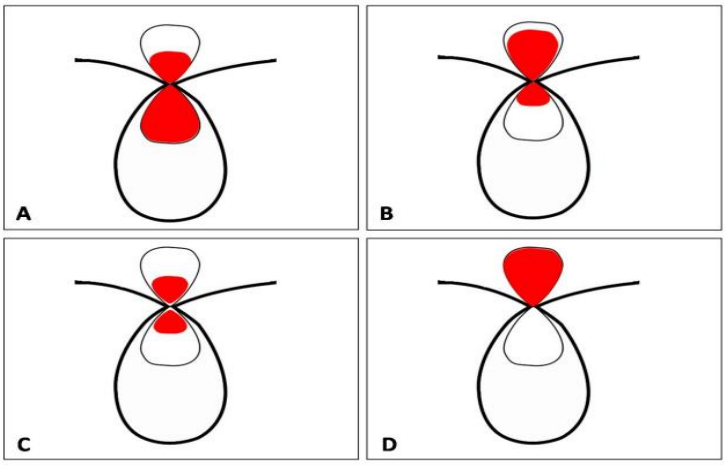

(a)

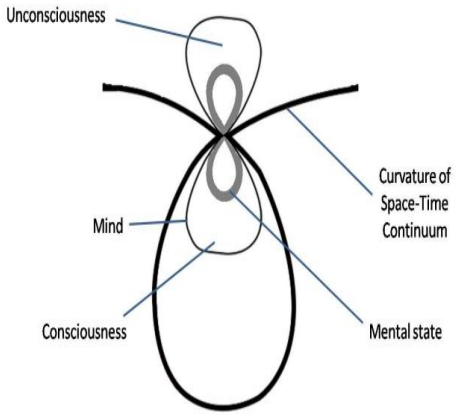

(b)

Figure 29 (a) The various mental states of man, based on hourglass theory. The red shapes show the mental state in various conditions: A: Fully awake, B: Asleep, C: Schizophrenia, D: Death (b) the parts and subparts of the mind within the space-time curvature shaping a hourglass structure (adopted from ref. Assadi [69])

Assuming the "mental state" as the sand Assadi considered the size of the filled space is located within this sand which indicates our mental state that vary at every moment like sand is passing through the narrow tunnel connecting these two bulbs. This mental state is the "mental capacity". Basically, the sand tends to move to the upper bulb i.e. "unconsciousness" through enough energy provided by the neuronal activity of the brain tries to keep it at the lower bulb (Figure 29 a). Like our various mental states this hourglass shifts upward or downward. For example, in asleep state it moves upward and in downward when awakening. This implies that a "decrease, increase or modified forms.

Regarding consciousness, when we are reading a book means we are almost aware of conscious, but we remain unaware of our conscious as well as do not know what is restoring in our unconsciousness. On the other hand, when we go to bed and sleep is coming implies that our consciousness level decreases i.e. it can be said that the mental capacity gradually moves from lower section to the upper bulb section. Comparing to the sand it will continue as much as some remains in the lower section and for this reason a loud sound or painful stimuli makes us awake. Note that "Coma" phase / state indicates the amount which is as less as it does not easily return to consciousness. Precisely, it is the condition when the brain is biologically incapable or not strong enough to do so. Here, Schizophrenia phase is considered as a state of separation of the

patient from the reality, morality, learned norms when a junction is so narrow and hard movement of the mental capacity two section (Figure 29 b).

So, death would be a situation of total shift of the capacity upwards, and the narrow junction is active such that prohibiting the return (Figure 29 d).

7.Time Reversal

7.1 Time Reversal in Cosmic Scenario

Short Gamma Ray bursts (SGRBs) are considered as the most luminous explosion events in the universe. But origin of such bursts is not yet fully known. It is believed that the most promising scenarios are associated with the merging of binary neutron stars (NS-NS) system and also the neutron star-black hole (NS-BH) mergers [70, 71]. It is generally assumed that within $\lesssim$ 100 ms after the merger the formation of Black hole torus (i.e. BH-torus) is responsible for the generation of SGRB emission that lasts $\lesssim$ 2 s [72]. Analysis of the long lasting "plateau-shaped" X-ray after-glows (detected by the Swift space-based satellite) indicates a supply of energy injected by a central engine for a period of time scale up to ~ 10s [73]. This implies that a magnetic spin down radiation from an (in) definitely stable neutron star formed through a binary NS merger [74]. Other observations of high mass neutron star with a rather stiff equation of state [75] suggest the possibility of formation of a long-lived or even stable neutron star in the binary neutron star (BNS) merger events. Thus, the existence of long lasting, sustained X-ray afterglow produced in the NS-BH progenitor scenario offers a challenge because of a single neutron star can be formed in this case.

In this context, Ciolfi and Siegel [76] proposed a new scenario, assuming a BNS produces a long-lived NS such that it emits spin down radiation and eventually collapses to a "BH-torus" system that is capable to explain this puzzles i.e. why the X-ray emission, powered by the NS spin, is observed after the prompt SGRB emission.

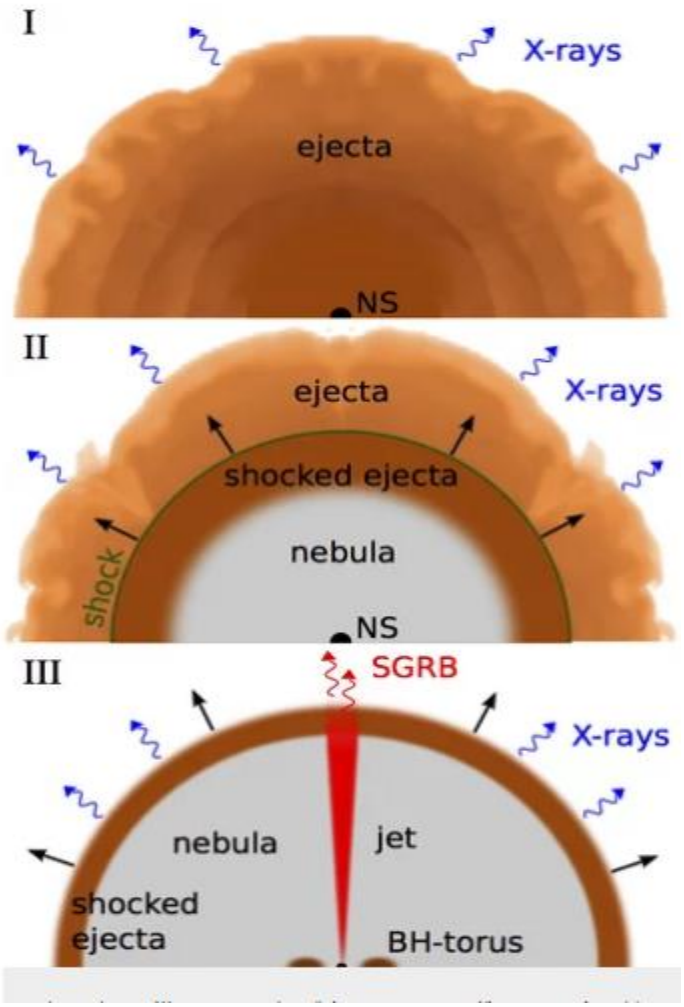

Figure 30: illustrate the "time-reversal" scenario indicating (I) a differentially rotating neutron star (NS) ejects a wind of NS matter. (II) When the star has settled down to uniform rotation, it generates a nebula of electrons, positrons and photons that inflates the previously ejected matter (shock). (III) The NS collapses to a black hole (BH) with an accretion disk (torus) and generates a short gamma-ray burst (adopted from ref. [76])

Figure 30 shows a simple schematic diagram of time reversal scenario model. In this model the merger remnant is a supra-massive neutron star (i.e. neutron star mass lies within the range-above the maximum mass for non-rotating configuration (M_{TOV}) but below the maximum mass for uniformly rotating configuration i.e. $M_{max} \approx 1.15\text{-}1.20\ M_{TOV}$). Observations show the NS masses as large as $\cong 2\ M_{\odot}$ and the supra-massive NS, originated from binary NS as merger remnant are very likely possible [75, 77]. In a merger magnetic field amplification, mass ejection associated with it, baryon loaded winds are produced due to either by large magnetic pressure gradient at the surface (see Figure 30 I) [78, 79] or induced by neutrino emission [80]. After the merger remnant settled down to a uniformly rotating, strongly magnetized neutron star further mass ejection is suppressed. In this phase NS again starts to emit electromagnetic (EM) spin down radiation (see Figure 30 II). This spin down emission thus inflates a photon-pair plasma nebula [81] behind the expanding ejecta. The high photon pressure drives a strong shock through the ejecta, resulting which it sweeps up the material into the formation of thin shell. The rapid propagation towards the outer ejecta radius, a shock breaks out following a transient signal observed in the form of early precursor to SGRBs [82].

Nebula energy is deposited in the optically thick ejecta causing a conversion into thermal and kinetic energy, such that a rapid acceleration of the ejecta helps to achieve the relativistic speed [83]. Now a situation will arise when rotation can no longer prevent the NS from its collapsing to BH i.e. within millisecond time scale a BH-torus system forms. According to Ciolfi and Siegel [76] this BH-torus generates suitable condition for producing the prompt SGRBs emission (see Figure 30 III). In this case the jet can easily pass through the surrounding photon-pair plasma and baryon-loaded ejecta before the NS collapse but it diffuses outward taking a much longer time scale implying a significant delay before the final escaping. In other words, this delay clearly explains;

(i) How the X-ray powered by spin down radiation before the collapse as observed in part before and in part after the prompt emission;
(ii) The optically thick nebula ejecta is collectively responsible for a “time reversal” in the observed emitting signals.

7.2 Time reversal in human embryos early in development

In general, the known fact is as we grown up i.e. aged, all of our body cells accumulate damage over time. The mystery is our offspring do not inherit such change (i.e. parents’ age) when the child is born. This means that child’s age is zero when they are born i.e. an immortality of germline cells such as eggs or sperm. Scientists believed that germline cells might be ageless so that they are somehow protected from the passage of time.

Recent study [84] shows that signs of aging in eggs and sperms. This study offers:

i) To dispel our earlier idea;
ii) To rethink for a new hypothesis-indicating that germline cells might reset their age after conception i.e. Reversing any damage.

In this recent study scientists found evidence that supports a new hypothesis, so called rejuvenation hypothesis, such that human germline cells appear to reset their biological age in the early stages of the development of an embryo (figure 31). This rejuvenation period or time begins just after the attachment of an embryo to the uterus that sets the growing embryo at its youngest biological age, counting as “ground zero”. Although the physics of this is not yet clear, scientists are trying to resolve the puzzle.

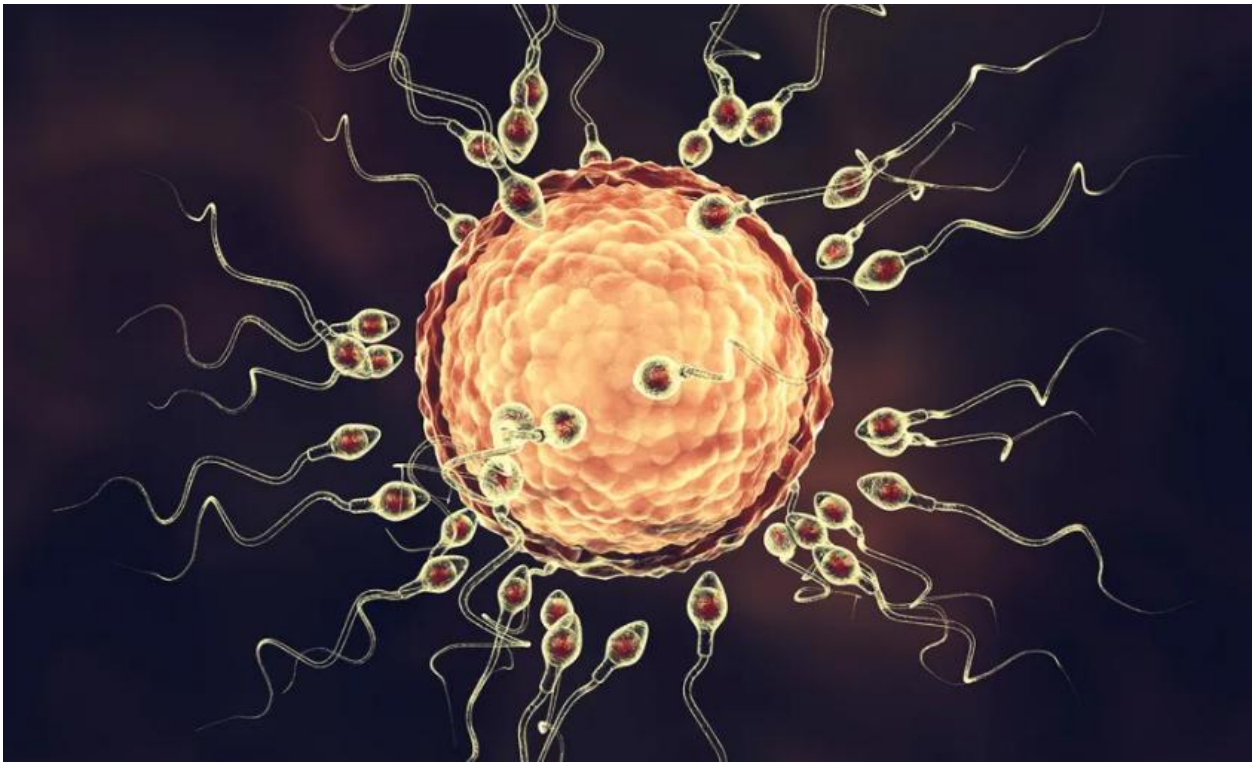

Figure 31: illustrates the picture of a human egg is surrounded by the sperm but after formation of human embryo how it reset the biological age during its development remains still unknown (adopted from ref. Kerepesi et al [84]; Courtesy-Science Advances 25th June 2021 and Katerynakon / Science photo library)

8.Conclusion

Gravity plays an important role in the formation of stellar objects. Einstein's general theory of relativity provides two ideas-(a) emission of gravitational waves and (b) ripples in space-time. Origin of gravitational wave in stellar objects may be due to high-speed rotation, strong internal magnetic fields of the stars. Generation of ripples in space-time means the motion in space time implies that stellar baby objects can have a similar type feeling as that of in human baby.

Fertilization i.e. how and when the egg and sperm combine inside a mother's womb is an invisible or undetected part till today. Initially, the gestational sac, located slightly paracentrically in the decidue, remains out of USG range but its rapid growth (~ 1mm per day) such that when it (i.e. the gestational sac) becomes a mean diameter of 2-4 mm, then its borders appear echogenic i.e. detectable in ultrasonography. The ultrasonographic image of gestational sac at about week 5 shows the elliptical shape of the gestational sac with the appearance of the yolk and embryo. Further development of this embryo with the developed parts of the human baby can be observed through USG. The echography of stellar baby also provides various phases or states of a baby star from its conception to birth. Comparative study of the characteristics of human baby and baby star (below table I) shows the formation issue i.e. zygote formation is the starting or initial phase of human baby has a similar one of the contraction phase in baby star. During evolution the gestational sac changes into elliptical shape from its circular shape in order to give space for the growth of embryo. In the case of binary system mass feeding makes its envelope into elliptical shape. Occasionally, twin baby forms inside the mother's womb instead of single baby in general as well as very rare conjunction baby.

Table I: Comparative study of the characteristics of human baby with the baby star

Particulars / facts	Human Baby	Baby Star
lll Embryo Formation	Zygote formation from the combination of the egg and sperm	Conception of ISM gas and dust
Umbilical Cord	Approx. .50 cm (i.e.20 inch) long and approx. .2 cm (i.e.0.75 inch) diameter	~ 500 Pc (1Pc = the distance travelled by light in one year)
Elliptical Shape	The shape of the gestational sac is more elliptical than circular	Deformation of spherical shape due rotation, strong internal magnetic field.
Birth span time	Approx.40 weeks required (i.e.1^{st} + 2^{nd} + 3^{rd} trimesters).	About million years
Heart Beats	During first month ~ 75-80 beats per minute (BPM) and highest at 165-185 BPM at 7^{th} week. At developed / growth stage of the fetus the ratio comes to 110-160 BPM.	Decoding of the observed data indicates heart beats of baby stars are detected. This beats from young stars provide a new chronometer for stellar evolution
First Cry	After delivery baby's first cry is crucial indicating health is OK and capable of adjusting with outside atmosphere	Astronomers found a similar like first cry in baby star

Sneeze	An usual fact that can observe in baby after delivery	A similar type fact also happens in baby star case also
Twin	Twin baby is possible. They are like normal single baby in two numbers that can form, grow in mother's womb and finally took birth. This happens occasionally.	Binary star i.e. two stars are under same envelope but origin is not yet clear. Majority of the massive stars are in binary system.
Conjugate Baby	Twin baby but some body-parts are joint with each other	Contact binaries are the same type in which two stars are in contract state
Ultrasonography	Analysis of the USG images indicates that in pregnancy a) first trimester i.e. the first 12 weeks is a crucial time for fetal development. Major organs and structures develop, heart beat is regular, nerves and muscles work together, eye lids found but remain close. b) In Second trimester: fetus movement i.e. sucking motion, regular sleeping, waking can observe. c) In 3rd trimester: Lung, eyes, and other body parts fully work, bones are hardening, fetus drops in the lower abdomen with head down ward position	Decoded or animated model of the pre-life story of a star (like sun) provides a time span of about 10 million years from conception to birth. Different points of the evolution or growth of a stellar embryo can be estimated.
Hourglass shape	Hourglass structure is observed in female body figure. Proteins i.e. Aquaporin, located inside the human eye, form an hourglass shape. Human mind and emotion both follow the Hourglass shape.	Hourglass structure is observable in the cosmic objects from star formation to galaxy

In case of massive stars ($\geq$ 10 M_o, M_o being the solar mass) majority of them are born in binary system or higher order multiple systems [55, 56]. Contact binaries have a similarity with that of conjugate human baby. Regarding new born baby human baby, first cry is the most priority after delivery in order to symbol of healthy baby who has adjusted with the surrounding atmosphere. Sneeze also another characteristic of a new born baby. Decoding of the observed parameters hints that stellar baby also suffers from cry, sneeze, etc. Not only that, heart beats also present both in the cases of human baby and baby star. The significance of the above behaviors provides the clues for the characteristics of star's baby can also be application to find the origin of similar characteristics observed in human baby.

Hourglass shape is an important fact that appears in compact objects and in human body. Regarding compact objects scientists have revealed the same during various phases in their evolution such that star formation, proto-star phase, dying phase. In the case of human, this hourglass structure is observed in few women bodies (not for all women) at their grown up age.

Time reversal is another mysterious, puzzling phenomenon that each and every human embryo have to cross. But the physics of its origin not yet clear to us. Scientists count the ground zero age of an human embryo when it stacks in the gestational sac though the embryo forms from the old, aged egg and sperm. The mechanism how embryos transform themselves by reversing the old age into fresh new age not yet known till date.

Therefore, "Time Reversal" is an inevitable, significant scenario that must appear human embryo in their early phase while binary NS-NS and NS-BH mergers emit short gamma ray bursts as evidence of time reversal occurring.

Based on the above supporting phenomena this author suggests that;

a. Stars' babies and human babies both exhibit a similar type characteristic;
b. Cosmic connection might be present in human that has not yet been discovered;
c. These (in) direct evidences favour the origin of life in space;
d. Triaxiality during embryo's early development phase might have a significant role towards the formation of hourglass body shape structure and ageless appearance in human body.

Acknowledgement

The author is greatly indebted to Prof. H. N. K. Sarma, Dept. of Physics, Manipur University; Mr B K Ganguly, Airports Authority of India, Kolkata. He also wishes to thank Mrs. Tapati Parui and Mr Rajarshi Parui for their various helps.

Data Availability: Data sharing is not applicable as no datasets were used / analyzed. **Declaration:**

Competing Interest: The author declares no competing interests.

Ethical Conduct: Not applicable

References

[1] S. Ray: The man who listened to plants, Reading Jagadish Chandra Bose's botanical language. Orion Magazine. http://orionmagazine.org/article/jagadish-chandra-bose-botanist-plant-language. (2023)
[2] A. Sinha: New study says plants "cry out" when distressed: Recalling Jagadish Chandra Bose's work on this a century ago. Indian Express (20 April 2023)
[3] P. K. Tandon: Jagadish Chandra Bose & Plant Neurobiology. Indian J. Med. Research.1**49**, 593 (2019)
[4] A. Einstein: Academie der wissenchaften Zu Berlin **1915**, 844 (1915)
[5] A. Einstein: Annalen der Phys.3**54**, 769 (1916)
[6] B. P. Abbott et al. (LIGO Scientific Collaboration and Virgo Collaboration): "Observation of Gravitational Waves from a Binary Black Hole Merger". Phys. Rev. Lett.1**16**, 061102. (2016) doi: 10.1103/PhysRevLett.116.061102
[7] N. Robert: Gravitational Wave detection heralds new era of science. Sky & Telescope (11th Feb.2016)
[8] NANOGrav.2023: The NANOGrav Collaboration: Focus on NANOGrav's 15 years Data set and the Gravitational Wave background (June 2023). http://iopscience. iop. org/collections/april-230623-245-Focus-on-NANOGrav-15-year.
[9] G. Agazie, A. Anumarlapudi, A. M. Archibald, P. T. Baker, B. Becsy, B. Blecha, et al.:
[10] The NANOGrav 15 yr Data set: Constraints on Supermassive Black hole Binaries from the gravitational wave background. Astrophys. J. Lett.9**52**, L37 (2023a):
[11] The NANOGrav 15 yr Data Set: Evidence for a Gravitational-wave Background e Astrophys. J. Lett., **951**, L8 (2023b) doi. org/10.3847/2041-8213/acdac6
[12] The NANOGrav 15 yr Data Set: Observations and Timing of 68 Millisecond Pulsars. Astrophys. J. Lett.9**51**, L9 (2023c) doi. org/10.3847/2041-8213/acda9a
[13] The NANOGrav 15 yr Data Set: Search for Anisotropy in Gravitational Wave Background. Astrophys. J. Lett.9**56,** L3 (2023d)
[14] D. Richstone, E. A. Ajhar, R. Bender, et al.: Supermassive black holes and the evolution of galaxies. Nature **385**, A14 (1998)
[15] J. P. Ostriker, M. A. Hausman. : Cannibalism among the galaxies: Dynamically produced evolution of cluster luminosity functions. Astrophysical Journal.2**17**, L125 (1977)
[16] C. Lacey, S. Cole: Merger rates in hierarchical models of galaxy formation. MNRAS **262**, 627 (1993)
[17] M. Milosavljevic, D. Merritt: Formation of Galactic Nuclei. Astrophys. J.5**63**, 34 (2001)
[18] N. Gehrel, G. Chincarini, P. Giommi, et al.: The Swift Gamma Ray Bursts Mission.
[19] Astrophys. J**.611**, 1005 (2004)
[20] N. Gehrels, S. Razzaque: Gamma Ray Bursts in the Swift Fermi Era. Frontiers Phys.8**,** 661-678 (2013)
[21] P. A. Evans, J. D. Gropp, J. A. Kennea, N. J. Klinger, et al.: Swift BAT trigger 960986: Swift detection of a new SGR Swift J1818.0-1607. GCN **circular # 27373** (2020)
[22] P. Esposito, N. Rea, A. Borghese, F. C. Zelati, D. Vigano, et al.: A very young radio-loud Magnetar. Astrophys. J. Lett.8**96,** L30 (2020)
[23] D. Champion, G. Desvignes, F. Jankowski: Spin evolution of the new magnetar J1818.0-1607. **Astron. Telegram # 13559** (2020)
[24] R. K. Parui: A Remark on "Do triaxial supermassive compact star exist?". Int. Astron. Astrophys. Res. J.5, 33 (2023)
[25] R. K. Parui: A New Compact Star-the Triaxial Star-and the detection of a Cosmic Baby: A possibility. Int. Astron. Astrophys. Res. J.5, 38 (2023)
[26] R. K. Parui: Cosmic Baby and the detection of a new compact star-the Triaxial Star: A possibility. Astrophys. Sp. Sci.3**68**, 46 (2023) Revised version is under preparation and to be submitted to Astrophys. Sp. Sci. (2024)
[27] B. B. Zhang, Z-J. Zhang, J-H. Zou, X. Wang, et al.: A hyperflare of a weeks-old magnetar born from a binary neutron star merger. arxiv: 2205.07670 (2022)
[28] R. K. Parui: Cosmic Baby and detection of a Neo-Natar Triaxial Star: A possibility. A Revised manuscript to be submitted to Euro. Phys. J. C (2025)
[29] R. K. Parui: Commentary on "Cosmic Baby and the Detection of a New Compact Star -the "Triaxial Star": A Possibility". J. Nanotechnol. Nanomaterials.5, 56-60 (2024)
[30] A. A. Hegazy: Anatomy and embryology of umbilicus in newborns: A review and clinical correlations. Front. Med.1**0**, 271 (2016)
[31] W. H. Persutte, J. Hobbins: Single umbilical artery: a clinical enigma in modern prenatal diagnosis. Ultrasound Obstet. Gynecol.6, 213 (1995)
[32] K. M. Rathbun, J. P. Hildebrand: Placenta Abnormalities. StatPearls [internet], StatPearls Publishing, Treasure Island, USA (2022)
[33] M. Moshiri, S. F. Zaidi, T. J. Robinson et al.: Comprehensive imaging review of abnormalities of the umbilical cord. Radiographics **34**, 179 (2014)
[34] J. R. Heil, B. Bordoni: Umbilical Cord. Embryology (17th April 2023)
[35] H. S. Hosseini, K. E. Garcia, L. A. Taber: A New hypothesis for foregut and heat tube formation based on differential growth and actomyosin contraction. Development **144**, 2381-2391 (2017)
[36] R. H. Anderson, S. Webb, N. A. Brown, W. Lamers, A. Moorman: Development of the Heart: II Separation of the atriums and ventricles. Heart **89**, 949-958 (2003)
[37] GLWM: Chapter 4. Ultrasound in the first Trimester in The Global Library of Women's Medicine 678 (2013)

[38] V. A. Murugan, B. O'Sullivan Murphy, C. Dupuis, A. Goldstein, Y-H. Kim: Role of
[39] ultrasound in the evaluation of first-trimester pregnancies in the acute setting. Ultrasonography **39**, 178 (2020) doi. org/10.14366/usg.19043
[40] M. Bethune, E. Alibrahim, B. Davies, E. Yong: A Pictorial guide for the second trimester ultrasound. Australas J. Ultrasound Med.1**6**, 98 (2013) doi. org/10.1002/j.2205-0140.2013. tb00106. x
[41] K. J. Gough: Third trimester ultrasound pictures. American Institute of Ultrasound in Medicine -AIUM. org (2023)
[42] A. Khalil, A. Sotiriadis, F. D'Antonio, F. Da Silva Costa. et al.: ISUOG Practice Guidelines: Performance of 3rd Trimester obstetric ultrasound scan. Ultrasound in Obstetrics & Gynecology **63**, 131 (2024)
[43] K. J. Gough: Take a sneak peak at your baby's development with this slideshow of ultrasound pictures from the third trimester of pregnancy. Blog.26th June 2023 (2023)
[44] Z. Schutte, A. E. Reines: Black hole-triggered star formation in the dwarf-galaxy Henize 2-10. Nature **601**, 328 (2022). Doi: 10.1038/s41586-021-04215-6
[45] Q-C. Shui, S. Zhang, J-Q. Peng, et al.: A phas resolved view of "Heart Beat"-like variability in IGR J17091-3624 during the 2022 outburst. Astrophys. J. arXiv: 2407.19388 {astro-ph. HE]
[46] K. Zwinty, L. Fossati, W. W. Weiss: Ecography of young stars reveals their evolution. Science.3**45**, 550-563 (2014).
[47] MOST Space Telescope: "Ultrasound" of baby stars per fared using Canada"s MOST space Telescope. UBC Phys. Astron. (9th July 2014)
[48] J. J. Tobin, J. Chandler, D. J. Wilmer, L. W. Looney, et al.: VLA and CARMA observations of proto-starsin the Cepheus clouds: Sub arcsecond photo-binaries formed via disk fragmentation. Astrophys. J.7**79**, 93 (2011)
[49] R. Boyle: Binary stars that found like fraternal twins. New Scientist (14th January 2014)
[50] M. J. Thompson: An Introduction to Astrophysical fluid dynamics. Imperial College Press, London. P.51-53 (2006). ISBN: 1-86094-615-1
[51] G. P. Kuper: On the interpretation of beta-Lyrae and other close binaries. Astrophys. J.9**3**, 133 (1941)
[52] J. Mullaney: Double and Multiple stars and how to observe them, Springer, NY, London. P.19 (2005). ISBN: 1-85233-751-6
[53] N. Ivanova, et al.: Common envelope evolution: where we stand and how we can move forward. Astron. Astrophys. Review.2**1**, 59 (2013)
[54] CXO 2000: Chandra X-ray Observatory, X-ray snapshots capture the First Cries of Baby Stars. Press Release CXCPR: 00-27 (08th November 2000)
[55] C. Wanjik: First cries of Baby Stars. Sci. News.31st October 2000.
[56] Kyushu University 2024: Kyushu University, Researchers in baby stars discharge Plume-like "sneezes" of magnetic flux during formation. Phys. Org (11th April 2024)
[57] W. C. Chen: Constraining the ellipticity of millisecond pulsars with observed spin down rates. Phys. Rev. D **102**, 043020 (2020)
[58] J. C. N. de Araujo, J. G. Coelho, C. A. Costa: Gravitational waves from pulsars in the context of magnetic ellipticity. Euro. Phys. J. C **77,** 350 (2017).
[59] W. C. Chau, K. S. Cheng, J. L. Zhiang: Remarks on Triaxiality spin up and magnetic field obliquity of some millisecond pulsars. Astrophys. J**.390**, 486 (1992)
[60] D. Luo, R. McCray: The Circumstellar shell of SN1987A. Astrophys. J.3**79**, 659 (1991)
[61] R. Sahai, A Dayal, A. M. Watson, et al.: The etched hourglass nebula MyCn 18. I. Hubble Space Telescope observations. Astrophys. J.1**18**, 468 (2007)
[62] J. I. Arias, R. H. Barba, M. Apellaniaz, N. Morrell, M. Rubio: The infrared Hourglass cluster in M8. MNRAS **366**, 739 (2006)
[63] B. Link, R. I. Epstein: Precession Interpretation of the Isolated Pulsar PSR B1828-11. Astrophys. J.5**56**, 392 (2001)
[64] N. Hurley-Walker, N. Rea, S. J. McSweeney, B. W. Meyers, E. Lenc, I. Heywood, S. D. Hyman, et al.: A long-period radio transient active for three decades. Nature **619**, 487-490 (2023)
[65] K. Qiu, Q. Zhang, K. M. Menten, H. B. Liu, Y-W. Tang, J. M. Girart: Submillimeter Array Observations of Magnetic Fields in G240.31+0.07: an Hourglass in a Massive Cluster-forming Core. Astrophys. J.7**94**, L18 (2014)
[66] I. W. Stephens, L. W. Looney, W. Kwon, et al.: The Magnetic Field Morphology of the Class 0 Protostar L1157-mm. Astrophys. J. Lett.7**69**, L15 (2013)
[67] N. M. H. Vayet, A. P. Rushton, M. Lloyd, J. A. López, J. Meaburn, T. J. O'Brien, D. L. Mitchell, D. Pollacco: High-speed knots in the hourglass-shaped planetary nebula Hubble 12. MNRAS **398**, 385-393. (2009)
[68] O. Gottlieb, H. Nagakura, A. Tchekhovskoy, et al.: Jetted and Turbulent stellsr deaths: New LVK-detectable Gravitational Wave sources. Astrophys. J. Lett.9**51**, L30 (2023)
[69] Francis Reddy, NASA's Scientific Visualization Studio (2018)
[70] R. M. Crocker, et al.: Gamma-ray emission from the Sagittarius dwarf spheroidal galaxy due to millisecond pulsars. Nature Astron, published online September 5, 2022; doi: 10.1038/s41550-022-01777-x
[71] H. -Y. Karen Yang, M. Ruszkowski, E. Zweibel: Fermi and eRosita bubbles as relics of the past activity of the Galactic black hole. Nature Astronomy **6,** 584-591 (2022)
[72] International GEMINI Observatory: Celestial Hourglass-Gemini South telescope captures exquisite planetary nebula (20 February 2020)
[73] M. Alser, K. Naja, M. A Elrayess: Mechanisms of body fat distribution and gluteal-femoral fat protection against metabolic disorders. Frontiers in Nutr.1**1**, 1368966 (2024) doi: 10.3389/fnut.2024.1368966

[74] J. C. Hernández, F. Gomez, J. Stadheim, M. Perez, B. Bekele, K. Yu, T. Henning: Hourglass Body Shape Ideal Scale and disordered eating. Body Image.38, 85-94 (2021)
[75] R. Assadi: Mind an hourglass at the bed of time-space continuum. Phil Archive https://philarchive. org › archive › ASSMAH-2
[76] N. Gehrels, C. L. Sarazin, P. T. O'Brien, et al.: A short γ-ray burst apparently associated with an elliptical galaxy at redshift z = 0.225. Nature **437**, 851 (2005)
[77] L. Rezzolla, B. Giacomazzo, L. Baiotti, et al.: The missing link: Merging neutron stars naturally produce jet-like structures and can power short Gamma-Ray Bursts. Astrophys. J. Lett.7**32**, L6 (2011)
[78] V. Paschalidis, M. Ruiz, S. L. Shapiro: Relativistic simulations of black hole-neutron star coalescence: the jet emerges. Astrophys. J. Lett.8**16**, L14 **(**2015)
[79] B. P. Gompertz, P. T. O'Brien, G. A. Wynn: Magnetar powered GRBs: explaining the extended emission and X-ray plateau of short GRB light curves. MNRAS **438**, 240 (2014)
[80] B. D. Metzger, E. Quataert, T. A. Thompson, T. A. : Short-duration gamma-ray bursts with extended emission from protomagnetar spin-down. MNRAS **385**, 1455 (2008)
[81] J. Antoniadis, P. C. C. Freire, N. Wex, et al.: A Massive Pulsar in a Compact Relativistic Binary. Science **340**, 448 (2013)
[82] R. Ciolfi, D. M. Siegel: Short Gamma Ray Bursts in the "TIME-REVERSAL" Scenario. Astrophys. J.7**98**, L36 (2015)
[83] P. B. Demorest, T. Pennucci, S. M. Ransom, M. S. E. Roberts, J. W. T. Hessels: A two-solar-mass neutron star measured using Shapiro delay. Nature **467**, 1081 (2010)
[84] D. M. Siegel, R. Ciolfi, A. I. Harte, L. Rezzolla: Magnetorotational instability in relativistic hypermassive neutron stars. Phys. Rev. **D 87**, 121302 (R) (2013)
[85] K. Kiuchi, K. Kyutoku, Y. Sekiguchi, M. Shibata, T. Wada: High resolution numerical-relativity simulations for the merger of binary magnetized neutron stars Phys. Rev. **D 90**, 041502 (2014)
[86] L. Dessart, C. D. Ott, A. Burrows, S. Rosswog, E. Livne: Neutrino Signatures and the Neutrino-Driven Wind in Binary Neutron Star Mergers. Astrophys. J.6**90**, 1681 (2009)
[87] A. P. Lightman, A. A. Zdziarski: Pair production and Compton scattering in compact sources and comparison to observations of active galactic nuclei. Astrophys. J.3**19**, 643 (1987)
[88] E. Troja, S. Rosswog, N. Gehrels: Precursors of short gamma-ray bursts. Astrophys. J.7**23**, 1711 (2010)
[89] B. D. Metzger, A. L. Piro, A. L.: Optical and X-ray emission from stable millisecond magnetars formed from the merger of binary neutron stars. MNRAS **439**, 3916 (2014)
[90] C. Kerepesi, B. Zhang, S-G. Lee, A. Trapp, V. N. Gladyshev: Epigenetic clocks reveal a rejuvenation event during embryogenesis followed by aging. Science Advances.7, Issue 26, (2021) DOI: 10.1126/sciadv. abg6082